ORNL/TM-2020/1834

Analysis of PNAR Spent Fuel Safeguards Measurements Using the ORIGEN Data Analysis Module

Jianwei Hu
Germina Ilas
Ian Gauld

December 2020

**Approved for public release.
Distribution is unlimited.**

OAK RIDGE NATIONAL LABORATORY
MANAGED BY UT-BATTELLE FOR THE US DEPARTMENT OF ENERGY

DOCUMENT AVAILABILITY

Reports produced after January 1, 1996, are generally available free via US Department of Energy (DOE) SciTech Connect.

Website www.osti.gov

Reports produced before January 1, 1996, may be purchased by members of the public from the following source:

National Technical Information Service
5285 Port Royal Road
Springfield, VA 22161
Telephone 703-605-6000 (1-800-553-6847)
TDD 703-487-4639
Fax 703-605-6900
E-mail info@ntis.gov
Website http://classic.ntis.gov/

Reports are available to DOE employees, DOE contractors, Energy Technology Data Exchange representatives, and International Nuclear Information System representatives from the following source:

Office of Scientific and Technical Information
PO Box 62
Oak Ridge, TN 37831
Telephone 865-576-8401
Fax 865-576-5728
E-mail reports@osti.gov
Website http://www.osti.gov/contact.html

This report was prepared as an account of work sponsored by an agency of the United States Government. Neither the United States Government nor any agency thereof, nor any of their employees, makes any warranty, express or implied, or assumes any legal liability or responsibility for the accuracy, completeness, or usefulness of any information, apparatus, product, or process disclosed, or represents that its use would not infringe privately owned rights. Reference herein to any specific commercial product, process, or service by trade name, trademark, manufacturer, or otherwise, does not necessarily constitute or imply its endorsement, recommendation, or favoring by the United States Government or any agency thereof. The views and opinions of authors expressed herein do not necessarily state or reflect those of the United States Government or any agency thereof.

ORNL/TM-2020/1834

Nuclear Energy and Fuel Cycle Division

ANALYSIS OF PNAR SPENT FUEL SAFEGUARDS MEASUREMENTS USING THE ORIGEN DATA ANALYSIS MODULE

Jianwei Hu
Germina Ilas
Ian Gauld[1]

December 2020

Prepared by
OAK RIDGE NATIONAL LABORATORY
Oak Ridge, TN 37831-6283
managed by
UT-BATTELLE, LLC
for the
US DEPARTMENT OF ENERGY
under contract DE-AC05-00OR22725

[1] Retired from ORNL; work performed under contract with Spectra Tech, Inc., Oak Ridge, TN 37830

CONTENTS

LIST OF FIGURES iv
LIST OF TABLES iv
ABSTRACT 1
1. INTRODUCTION 1
2. PNAR MEASUREMENTS 2
3. METHOD FOR COMPUTATIONAL ANALYSIS OF PNAR MEASUREMENTS 5
3.1 GENERATION OF PNAR RESPONSE FUNCTIONS FOR ORIGEN MODULE 5
3.2 ORIGEN MODULE FOR ANALYSIS OF PNAR MEASUREMENT DATA 10
3.2.1 Neutron and Gamma Detector Count Rates 10
3.2.2 Net Neutron Multiplication 10
3.3 ADDITIONAL CONSIDERATIONS 11
3.4 GRAPHICAL USER INTERFACE (GUI) 12
4. COMPARISON OF CALCULATED AND MEASURED DATA 13
4.1 ANALYSIS USING SAFEGUARDS DATA 13
4.2 ANALYSIS USING OPERATOR DATA 17
5. UNCERTAINTY ANALYSIS 22
5.1 ISOTOPE CONCENTRATIONS 22
5.2 ASSEMBLY URANIUM MASS 24
5.3 INITIAL ^{235}U ENRICHMENT 24
5.4 BURNUP 24
5.5 MODERATOR DENSITY 25
5.6 COOLING TIME 26
5.7 OPERATING HISTORY 26
5.8 NET NEUTRON MULTIPLICATION 26
6. CONCLUSIONS AND RECOMMENDATIONS 28
ACKNOWLEDGMENTS 29
REFERENCES 29

LIST OF FIGURES

Figure 1. Axial profiles of burnup and moderator density for the BWR SVEA64 representative assembly and the axial profile of the calculated neutron emission rates. 7
Figure 2. Side view of the MCNP model of the PNAR measurement with an assembly in the middle (top part of the assembly is not shown here) (left); magnified view of the PNAR detector (upper right); top view of the MCNP model of the PNAR measurement (lower right). 8
Figure 3. Response functions for the PNAR neutron count rates for the SVEA64 assembly design. 9
Figure 4. Response functions for the PNAR gamma count rates for the SVEA64 assembly design. 10
Figure 5. Screenshot of the Java GUI for the ORIGEN Module for an example PNAR measurement analysis. 12
Figure 6. Part of the ORIGEN Module output file showing the calculated neutron and gamma count rates for a PNAR measurement. 13
Figure 5. The neutron count rate relative difference between the calculation (C) using safeguards data and PNAR measurement (M) for each assembly. 14
Figure 6. The gamma count rate relative difference between calculation (C) using safeguards data and PNAR measurement (M) for each assembly. 15
Figure 7. Calculated net neutron multiplication using safeguards data vs. measured PNAR ratio. The linear fit equation and the goodness of fit parameter (R^2) is also shown. 16
Figure 8. The relative differences between the calculated (C) PNAR neutron count rates using operator data and the measured (M) values for each assembly. 18
Figure 9. The relative difference between the calculated (C) PNAR gamma count rates using operator data and the measured (M) values for each assembly. 19
Figure 10. Calculated net neutron multiplication using operator data vs. measured PNAR ratio. The linear fit equation and the goodness of fit parameter (R^2) is also shown. 20
Figure 11. Comparison of nuclide contents predicted by ORIGEN and the SNF code for all measured assemblies. 23
Figure 12. Normalized burnup profiles of all measured assemblies (top) and relative standard deviation of the burnup (bottom) in each of the 25 axial nodes. Nodal burnup data were provided by TVO. 25
Figure 13. Assembly net neutron multiplication calculated by using the ORIGEN Module and MCNP. 27

LIST OF TABLES

Table 1. Assembly attributes and the measured PNAR Ratios and gross neutron and gamma count rates. 4
Table 2. The neutron and photon emission rate for each axial node of the BWR representative assembly with SVEA64 design. 6
Table 3. Calculated neutron count rates, gamma count rates, and *Mult* using the ORIGEN Module with safeguards data. 17
Table 4. Calculated neutron count rates, gamma count rates, and *Mult* using the ORIGEN Module with the operator data. 21
Table 5. Uncertainty analysis of predicted observables due to modeling uncertainty. 22

ABSTRACT

This report documents the analysis of the Passive Neutron Albedo Reactivity (PNAR) measurements for 23 boiling water reactor spent fuel assemblies that were performed in Finland under Action Sheet 65, which is an international collaboration on spent fuel safeguards verification methods in the context of the Finnish spent fuel encapsulation/repository system. PNAR measures the passive neutron and gamma emission rates from each of the spent fuel assemblies like a Fork detector, and it also measures the PNAR ratio, which is expected to correlate with the net neutron multiplication of the measured fuel assembly. The analysis was performed with the Oak Ridge Isotope Generation and Depletion (ORIGEN) Data Analysis Module, which was originally developed for predicting Fork detector spent fuel measurement signals in real time and has been integrated into the Integrated Review and Analysis Package developed by Euratom and the International Atomic Energy Agency. The module includes the ORIGEN burnup analysis code and integrates detector response functions pregenerated using the MCNP Monte Carlo transport code to predict the detector signals in several seconds per assembly. In this study, new response functions specific to the analyzed PNAR measurements were generated for the ORIGEN Module. The study also analyzes the impact of using detailed fuel design and operation information vs. standard safeguards information on the results calculated with the ORIGEN Module. Using detailed information reduced the standard deviation of the relative differences between calculated and measured neutron count rates among the 23 assemblies from ~10% to ~4%. The results obtained using standard safeguards information for these PNAR measurements were similar to those obtained for the Fork detector. A clear trend was found between the calculated net neutron multiplications and the measured PNAR ratios of the 23 assemblies. An uncertainty assessment of the calculations was also performed to estimate the potential impact of the accuracy and the completeness of declaration information on the calculated results for the count rates and net neutron multiplications. The ORIGEN Module predictions for PNAR signals and net neutron multiplication are expected to directly support the safeguards inspectors' efforts to verify operator declarations of a spent fuel assembly in real time in safeguards practices.

1. INTRODUCTION

Action Sheet 65 (AS-65) is a technical collaboration agreement signed in 2018 between the US Department of Energy (DOE)/National Nuclear Security Administration (NNSA)—represented by Los Alamos National Laboratory (LANL) and Oak Ridge National Laboratory (ORNL)—and the European Atomic Energy Community (Euratom) to collaborate on spent fuel safeguards verifications for the Finnish spent fuel repository. Under AS-65, measurements of 23 boiling water reactor (BWR) spent fuel assemblies were performed using the Passive Neutron Albedo Reactivity (PNAR) instrument in Finland in 2019. This report documents the analysis of the measurements using the ORIGEN Data Analysis Module.

The ORIGEN Module was originally developed to predict Fork detector spent fuel measurement signals in real time and has been integrated into the Integrated Review and Analysis Package (IRAP) developed by Euratom and the International Atomic Energy Agency [1]. This module includes the ORIGEN burnup analysis code distributed as part of the ORNL SCALE nuclear systems modeling and simulation suite [2] and integrates detector response functions pregenerated by using the Monte Carlo N-Particle (MCNP) code to predict the detector signals in several seconds per assembly. This module has been benchmarked against Fork measurement data for over 300 light water reactor assemblies [3]. The module was recently expanded to VVER-440 assemblies for Fork detector measurements [4] in addition to BWR and pressurized water reactor (PWR) assemblies. In this study, the ORIGEN Module was updated for PNAR by generating new response functions specific to the PNAR measurements.

This report focuses on using the expanded ORIGEN Module to analyze PNAR measurements for spent BWR assemblies. PNAR is one of the instruments that was studied and tested under NNSA's Spent Fuel Nondestructive Analysis project [5]. PNAR was further developed and tested by the Finnish Radiation and Nuclear Safety Authority (STUK) [6]. PNAR measures the neutron and gamma radiations from a spent fuel assembly by using ^{3}He tubes and ion chambers, respectively, and it typically measures a given assembly twice: with and without the presence of a Cd liner between the assembly and instrument. The ratio of the neutron signal without the Cd liner to that with the Cd liner is referred to as the *PNAR ratio*. Tobin et al. previously demonstrated primarily through MCNP simulations that the PNAR ratio is directly correlated with the net neutron multiplication of an assembly [6], which depends on the amount of fissile content and neutron absorbers present in an assembly. STUK measured 23 BWR assemblies in July 2019 in Finland [7]. Two datasets for the fuel design and operating conditions of these 23 assemblies were provided: (1) a set of basic data (e.g., assembly-average burnup, initial enrichments) similar to the operator declarations in a typical safeguards inspection (referred to as *safeguards data* in this report), which was provided by STUK and (2) a set of detailed data (e.g., detailed burnup and moderator density values along the height of the assemblies) provided by the reactor operator Teollisuuden Voima Oyj (TVO).

The ORIGEN Module expanded with the newly generated detector response functions was used in this study to predict the neutron and gamma signals from the PNAR measurements of the 23 BWR assemblies by using the safeguards data and the operator data for these assemblies. The net neutron multiplication was also calculated with the ORIGEN Module and compared with the measured PNAR ratio. This study also quantifies the uncertainties in the predicted neutron and gamma signals and the net neutron multiplication that are due to uncertainties in the input data for the ORIGEN Module (e.g., burnup, moderator density, initial enrichment).

By using pregenerated response functions, the ORIGEN Module can perform the burnup calculation and predict the neutron and gamma count rates and net neutron multiplication in seconds based on the operator declarations of a given spent fuel assembly, enabling inspectors to draw conclusions in real time on the correctness of the declarations. During a typical safeguards inspection, the operator declarations (e.g., the assembly-average burnup, initial enrichment, U mass, cooling time) for the assemblies to be measured are provided to the inspectors before the measurements. The safeguards inspectors use these declarations to perform the ORIGEN Module calculations during inspection and can compare the calculation results with the corresponding measured quantities and determine whether the operator declarations are consistent with the measured quantities, which provides a way to verify the identity and integrity of a subject fuel assembly.

This report briefly describes the PNAR measurements in Section 2, and Section 3 presents the computational analysis method and software used. Section 4 presents the results calculated by using safeguards and operator data and compares the calculated results with corresponding PNAR measured signals. Section 5 quantifies uncertainties in calculated results due to uncertainties in input parameters. Section 6 presents conclusions and recommendations.

2. PNAR MEASUREMENTS

The PNAR measurements were described in detail elsewhere [7], so only a brief summary is provided here. The PNAR measurements were made on 23 different BWR assemblies at the spent fuel interim storage facility at Olkiluoto Nuclear Power Plant by STUK in July 2019. The cooling times of these assemblies ranged from 6.2 to 35.1 years, and burnups ranged from 18,589 to 49,698 MWd/tU. The assemblies included several different assembly designs, including ones with part length rods. Three assemblies experienced operating histories in which they were removed from the core after irradiation, stored for one or more cycles, and reinserted in the core for further irradiation. All but two of the measured assemblies employed axial enrichment zoning.

The PNAR instrument, as illustrated in Section 3, has four neutron detectors and four gamma detectors, and the neutron and gamma detector count rates were acquired as one means of verification observables. These observables are similar to those acquired by the Fork detector measurements that are used for spent fuel verification. However, the PNAR system performs the neutron measurements in two different multiplying configurations: one with a Cd liner placed between the assembly and the detector and one without the Cd liner, to measure the PNAR ratio. The PNAR ratio is expected to correlate with the net neutron multiplication of the assembly, which is closely related to the inventory of fissionable material in the assembly. Therefore, in addition to acquiring the neutron and gamma signals like the Fork detector, PNAR provides a third measure related more directly to the assembly attributes of interest to safeguards authorities.

Measurements were made approximately 1.4 m from the bottom of the assembly. There are approximately 0.4 m of support structures and natural U at the bottom of the assembly below the enriched U zone [7]. The operator simulation data by TVO for these assemblies were provided for 25 equal-length axial nodes. Assuming that a natural U zone was present in the first bottom node (~15 cm) of most assemblies, the measurements were made ~115 cm above the bottom of the active fuel, which correspond to node 8 from the bottom of the assembly.

The key assembly parameters and measurement results (i.e., PNAR ratio, neutron and gamma count rates) for all measured assemblies are listed in Table 1. The numbering of these assemblies in the first column of Table 1 was kept consistent with the measurement report and is not continuous [7]. Also, neutron and gamma signals and PNAR ratios were averaged from only two opposite detector pods (2 and 4) instead of four pods in this work because pod 3 had a leak during the experiment [7]. This does not impact the adequate analysis of the signals because all four pods are in symmetric configurations. The uncertainty in the PNAR ratio reported in Table 1 includes only the counting statistics. The measurement report [7] indicates that the absolute standard deviation due to repeatability of the measurements is 0.0013. This source of measurement uncertainty was combined with the statistical counting uncertainty in the results presented in Section 4.

Table 1. Assembly attributes and the measured PNAR ratios and gross neutron and gamma count rates. PNAR ratios and gross count rates are averaged over two opposite detector pods (2 and 4). The reported standard deviation is only due to counting statistics.

Assembly #	Assembly type	Assembly lattice	Initial enrichment (wt % ^{235}U)	Burnup (MWd/tU)	Cooling time (year)	Continuous cycles	Part length rods	Axial enrichment zoning	PNAR ratio	PNAR ratio stdev (±)	Without Cd liner		With Cd liner	
											Neutron (cps)	Gamma (cps)	Neutron (cps)	Gamma (cps)
1	8 × 8-1	8 × 8	1.938	18,589	35.1	N	N/A	N	1.043	0.0026	701	9,2721	672	77,654
2	8 × 8-1	8 × 8	2.907	31,161	29.1	N	N/A	N	1.040	0.0017	3,190	176,222	3,068	147,698
3	SVEA-64	8 × 8	2.975	33,994	21.2	Y	N/A	Y	1.043	0.0011	7,777	279,365	7,458	238,146
4	SVEA-64	8 × 8	2.975	37,574	21.2	Y	N/A	Y	1.044	0.0009	10,825	298,677	10,367	255,188
5	SVEA-64	8 × 8	2.976	19,770	23.2	Y	N/A	Y	1.088	0.0032	970	163,324	891	136,646
6	SVEA-64	8 × 8	2.98	32,988	20.2	Y	N/A	Y	1.049	0.0011	7,195	278,921	6,858	238,031
11	SVEA-64	8 × 8	2.992	32,935	21.2	Y	N/A	Y	1.048	0.0012	6,767	271,823	6,459	231,667
13	SVEA-64	8 × 8	3.015	35,672	21.2	Y	N/A	Y	1.045	0.0010	9,322	293,573	8,920	250,657
18	9 × 9-1 AB	9 × 9	3.224	35,399	23.1	Y	N/A	Y	1.038	0.0012	6,349	246,719	6,119	209,677
20	ATRIUM10	10 × 10	3.231	37,107	17.2	Y	8 × 1/2	Y	1.049	0.0009	10,250	312,880	9,766	268,472
22	SVEA-100	10 × 10	3.235	37,604	19.2	Y	N/A	Y	1.044	0.0010	8,740	300,604	8,371	257,204
23	SVEA-64	8 × 8	2.975	33,919	21.2	Y	N/A	Y	1.044	0.0010	8,517	281,565	8,154	240,065
24	SVEA-64	8 × 8	2.976	33,175	21.2	Y	N/A	Y	1.044	0.0010	6,473	270,442	6,197	230,371
28	SVEA-64	8 × 8	2.989	32,581	21.2	N	N/A	Y	1.044	0.0010	6,230	251,253	5,966	213,386
30	9 × 9-1AB	9 × 9	3.22	35,043	21.1	Y	N/A	Y	1.046	0.0012	6,246	253,222	5,974	215,519
31	9 × 9-1AB	9 × 9	3.226	35,884	21.1	Y	N/A	Y	1.042	0.0012	6,084	251,833	5,837	214,346
35	SVEA-96	10 × 10	3.192	39,758	14.2	Y	8 × 2/3	Y	1.046	0.0008	15,694	394,146	14,998	339,125
39	ATRIUM10	10 × 10	3.22	35,039	17.2	Y	8 × 1/2	Y	1.054	0.0011	7,796	292,990	7,400	251,083
42	GE12	10 × 10	3.237	36,281	17.2	Y	14 × 2/3	Y	1.045	0.0011	8,771	304,521	8,391	261,028
43	GE12	10 × 10	3.245	43,088	12.2	Y	14 × 2/3	Y	1.039	0.0006	18,451	401,907	17,765	346,408
44	GE14	10 × 10	3.463	42,159	10.2	Y	14 × 2/3	Y	1.044	0.0007	20,794	472,094	19,912	408,063
46	GE14	10 × 10	3.521	43,312	6.2	Y	14 × 2/3	Y	1.049	0.0006	23,963	653,852	22,844	567,906
49	ATRIUM10	10 × 10	3.554	49,698	8.4	Y	8 × 1/2	Y	1.031	0.0005	30,164	492,139	29,267	425,731

3. METHOD FOR COMPUTATIONAL ANALYSIS OF PNAR MEASUREMENTS

The computational analysis of the PNAR measurement data in this study was performed by using the ORIGEN Data Analysis Module. This module includes the ORIGEN burnup analysis code, distributed as part of the SCALE nuclear systems modeling and simulation suite, version 6.1.2, and integrates detector response functions generated by using the MCNP code to predict the detector signals. This section summarizes the approach used for the analysis of the net neutron multiplication. This section also describes the generation of detector-specific response functions by using three-dimensional (3D) MCNP models of the PNAR detector system.

3.1 GENERATION OF PNAR RESPONSE FUNCTIONS FOR THE ORIGEN MODULE

The response functions record the MCNP-simulated detector responses due to a source neutron or photon particle emitted from the spent fuel. 3D MCNP models of the measurement system are needed to adequately calculate the PNAR detector response caused by a neutron or photon originated in the spent fuel assembly, given the axial and radial variations of burnup values, isotopic compositions, and radiation emission sources in the spent fuel assembly. Only the axial burnup profiles were considered for response function generation in this study because the radial burnup variation is not nearly as pronounced as the axial variations.

The assembly characteristics for the 23 measured assemblies listed in Table 1 show that 11 assemblies have an 8 × 8 fuel rod lattice (labeled “SVEA64” and “8 × 8-1”), three assemblies have a 9 × 9 lattice (labeled “9 × 9-1 AB”), and the other nine assemblies have a 10 × 10 lattice. Two BWR assembly designs were selected as representative for generating the spent fuel isotopic compositions and neutron/gamma source terms for use in the response function generation: (1) a SVEA64 design as representative for all 8 × 8 assemblies and (2) a SVEA100 design as representative for all 10 × 10 and 9 × 9 assemblies. Both representative BWR assemblies have a burnup of 35 GWd/tU, an initial enrichment of 3.0%, and a cooling time of 20 years.

The 3D spent fuel isotopic compositions and neutron and gamma source terms, which are needed in the response function generation, of the two representative BWR assemblies were calculated by using the ORIGAMI code in SCALE version 6.2.4 [8] based on user input for 25 node axial profiles of burnup and moderator density. Table 2 lists the input burnup and moderator density, as well as the calculated neutron emission and gamma emission rates for each of the 25 axial nodes (ordered from the bottom to the top of the assembly) of the representative assembly with the SVEA64 design. The results for the SVEA100 were similar to these, and they are not presented here.

Table 2. The neutron and photon emission rate for each axial node of the BWR representative assembly with SVEA64 design. The total initial U loading was assumed to be 0.18 MT.

BWR	Burnup (input)	Moderator density (input)	Neutron emission (output)	Photon emission (output)
Axial node	GWd/MTU	g/cm^3	rate (1/s)	rate (1/s)
1	12.5	0.761	1.69E + 04	1.49E + 13
2	28.0	0.754	3.75E + 05	3.17E + 13
3	34.3	0.735	9.73E + 05	3.80E + 13
4	37.0	0.700	1.47E + 06	4.05E + 13
5	38.6	0.655	1.87E + 06	4.21E + 13
6	39.4	0.607	2.12E + 06	4.28E + 13
7	39.7	0.562	2.28E + 06	4.31E + 13
8	39.7	0.520	2.29E + 06	4.30E + 13
9	40.1	0.481	2.54E + 06	4.34E + 13
10	40.2	0.447	2.65E + 06	4.35E + 13
11	40.2	0.416	2.72E + 06	4.34E + 13
12	39.9	0.389	2.70E + 06	4.31E + 13
13	40.1	0.365	2.77E + 06	4.34E + 13
14	40.0	0.344	2.87E + 06	4.32E + 13
15	39.9	0.325	2.88E + 06	4.31E + 13
16	39.6	0.309	2.82E + 06	4.27E + 13
17	39.6	0.294	2.86E + 06	4.27E + 13
18	39.1	0.281	2.71E + 06	4.23E + 13
19	38.4	0.269	2.60E + 06	4.16E + 13
20	37.3	0.258	2.34E + 06	4.05E + 13
21	35.7	0.249	1.98E + 06	3.89E + 13
22	33.1	0.241	1.47E + 06	3.63E + 13
23	28.6	0.235	7.90E + 05	3.18E + 13
24	21.1	0.225	2.29E + 05	2.39E + 13
25	13.1	0.214	3.72E + 04	1.52E + 13

Figure 1 compares the axial profiles of burnup, moderator density, and calculated neutron emission rate of the representative BWR assembly with SVEA64 design. As shown, the moderator densities decrease dramatically from the bottom to the top of the assembly along the vertical axis; the burnup is approximately symmetric around the centerline of the assembly. There is a pronounced peak of neutron emission in the midsection of the assembly due to the combined effects of higher burnups and lower moderator densities in that region. Lower moderator densities toward the top of the BWR assembly harden the flux spectrum during irradiation and lead to a greater production of actinides, including neutron source actinides, such as ^{244}Cm. Such drastically varying axial profiles in BWR assembly neutron emission rates are expected to significantly affect the PNAR neutron count rates, the extent of which depends on where the PNAR measurements are taken along the vertical axis of the assembly. Because the neutron source term is identical in the numerator and denominator of the PNAR ratio, the PNAR ratio is independent of the source term such as ^{244}Cm. As such, the PNAR ratio is expected to have less dependence on the axial variations of the neutron source term.

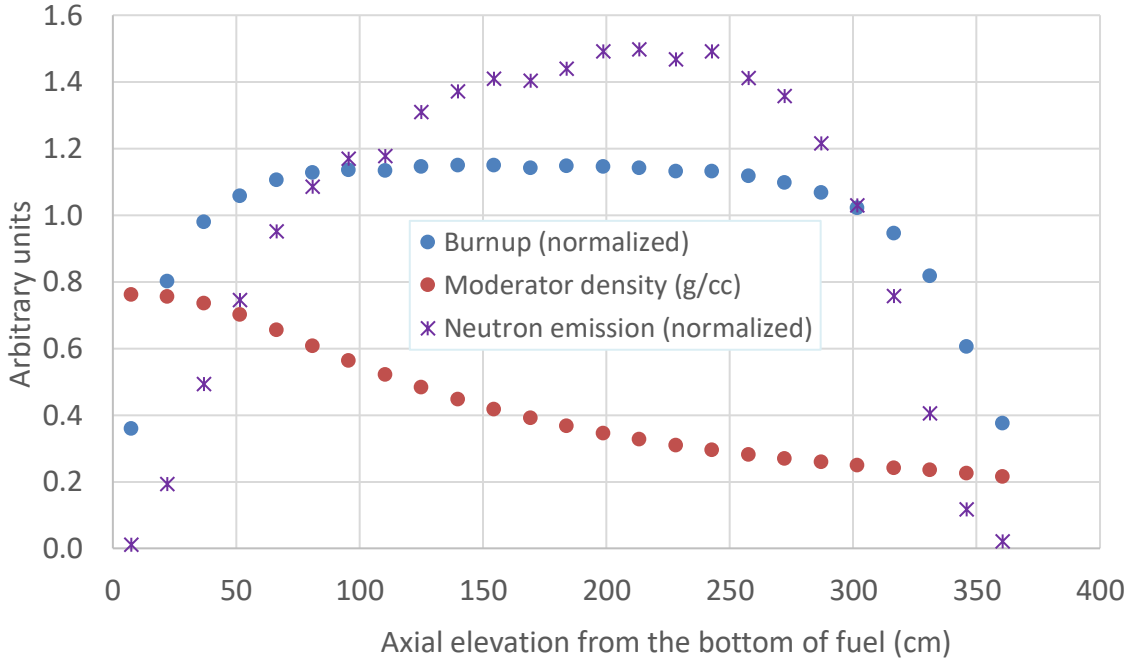

Figure 1. Axial profiles of burnup and moderator density for the BWR SVEA64 representative assembly and the axial profile of the calculated neutron emission rates.

The 3D MCNP model used to generate the response functions for the PNAR measurement of a SVEA64 spent fuel assembly, which is consistent with the actual configuration of the PNAR instrument used in Finland, is illustrated in Figure 2. The PNAR instrument is placed 100 cm above the bottom of active fuel. The top part of the assembly is not shown in the left of the figure due to limited space. The Cd liner is placed between the instrument and the fuel assembly in the "with Cd liner" case; the liner is moved 60 cm downward in the "without Cd liner" case, as labeled in this figure. There are four detector pods in PNAR, one on each side of the assembly. Each detector pod contains a ^{3}He tube for neutron detection and an LND 52110 ion chamber for gamma detections. More details of the PNAR instrument are found in other works [6].

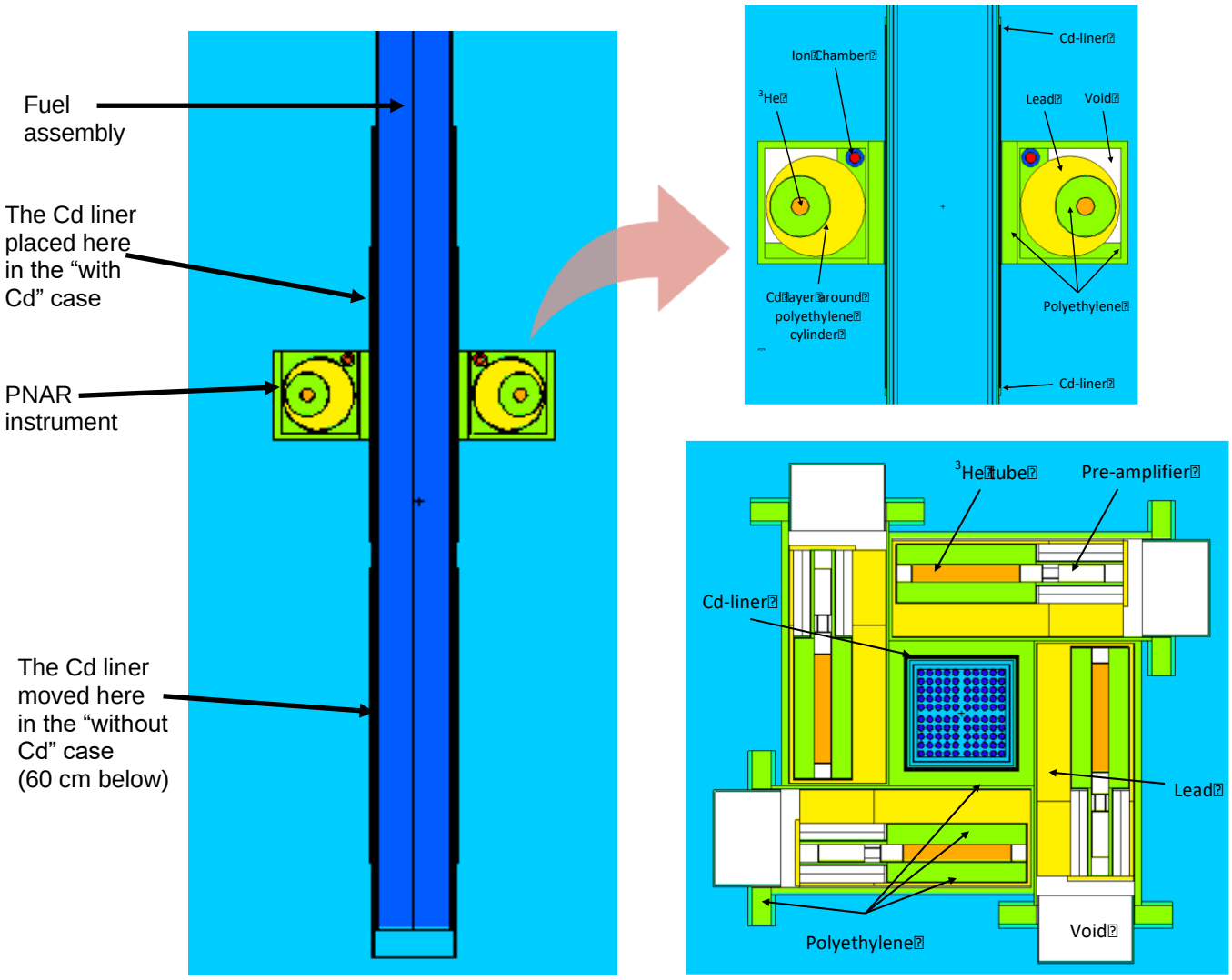

Figure 2. Side view of the MCNP model of the PNAR measurement with an assembly in the middle (top part of the assembly is not shown here) (left); magnified view of the PNAR detector (upper right); top view of the MCNP model of the PNAR measurement (lower right).

For the PNAR neutron response functions, 20 discrete source neutron energy bins were used to span 0.01–20 MeV with each energy bin simulated in a separate MCNP model. Since most neutrons are born at ~2 MeV in spent fuel, this neutron energy discretization is deemed sufficient. In each MCNP model, a fixed-source calculation was performed with MCNP6 (version 6.1) [9] with the neutron source particles sampled uniformly in the radial direction of the fuel assembly but nonuniformly in the axial direction based on the calculated neutron emission probability along the assembly axis (Figure 1). The neutron capture rates in the ^{3}He gas in all the PNAR ^{3}He tubes were tallied in these models to mimic the PNAR neutron count rates. A 2×10^8 particle history was used in the MCNP calculation for neutrons, which would take 43,000–58,000 min to complete on a single processor, depending on which source energy was used. This resulted in stochastic uncertainties in the calculated neutron response functions of <0.5% for all energy bins. The gamma count rates are calculated based on tallies for gamma dose rates deposited in the gas of the ion chamber, given that the gamma count rates are expected to be proportional to dose rates.

ANSI/ANS 1977 flux-to-dose factors [9] are used to convert gamma flux into dose rates. A 2×10^9 particle history was used in the MCNP calculations for the gammas, which would take 2,000–7,000 min to complete on a single processor, depending on which source energy was used. This resulted in stochastic uncertainties of <0.5% in the calculated gamma response functions for all energies but the lowest energy. The gamma dose deposited in the ion chamber work gas induces electric current, which is then converted to digital signals (i.e., count rates) by the PNAR data acquisition system.

Figure 3 illustrates the response functions for the PNAR neutron count rates for the modeled SVEA64 design. Neutron response functions for the "without Cd liner" case are 4–24% higher than those for the "with Cd liner" case at varying energies, which is expected because the Cd liner absorbs thermal neutrons returning to the assembly from surrounding materials and thus reduces induced fissions in the assembly. Figure 4 shows the response functions for the PNAR gamma count rates for the SVEA64 design. Gamma response functions for the "without Cd liner" case are 9–76% higher than those for the "with Cd liner" case at varying energies (except for 0.01 MeV); this is expected because the Cd liner, which has a higher density than that of water, further attenuates the gamma flux from assembly to the detectors. For 0.01 MeV, the gamma response function for the "without Cd liner" case is 8.65 times higher that of the "with Cd liner," which can be attributed to the higher shielding effect of the Cd liner for photons with lower energy. Response functions generated for the SVEA100 design were similar to the ones for the SVEA64 design, and they are not presented here.

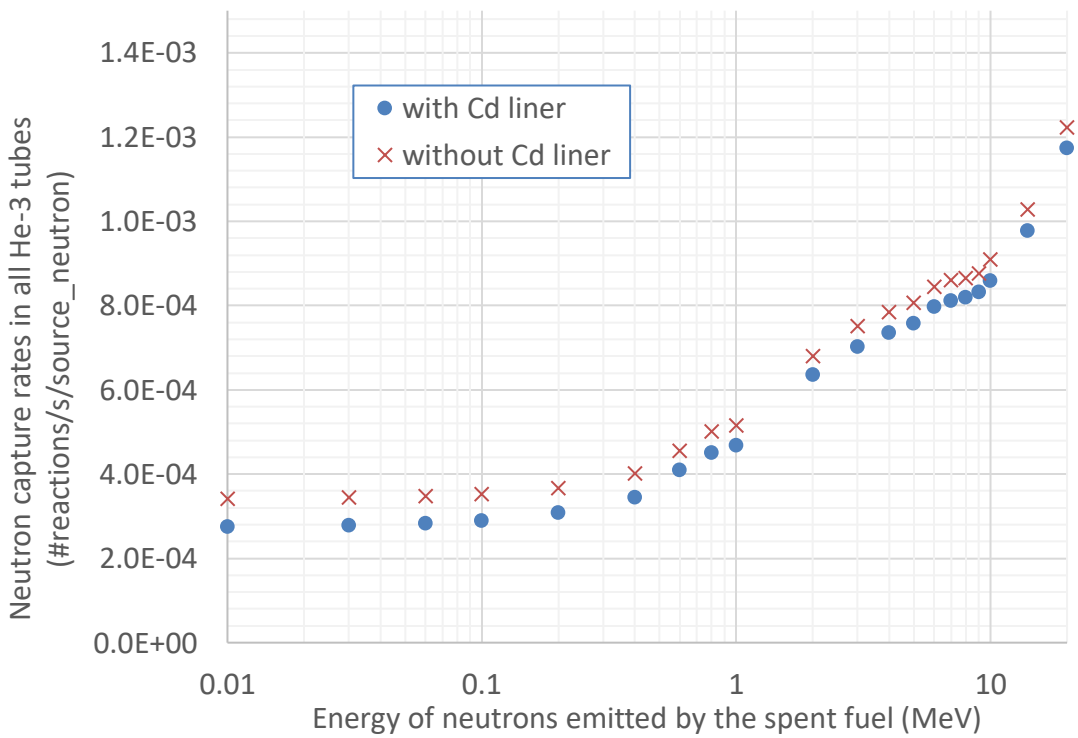

Figure 3. Response functions for the PNAR neutron count rates for the SVEA64 assembly design.

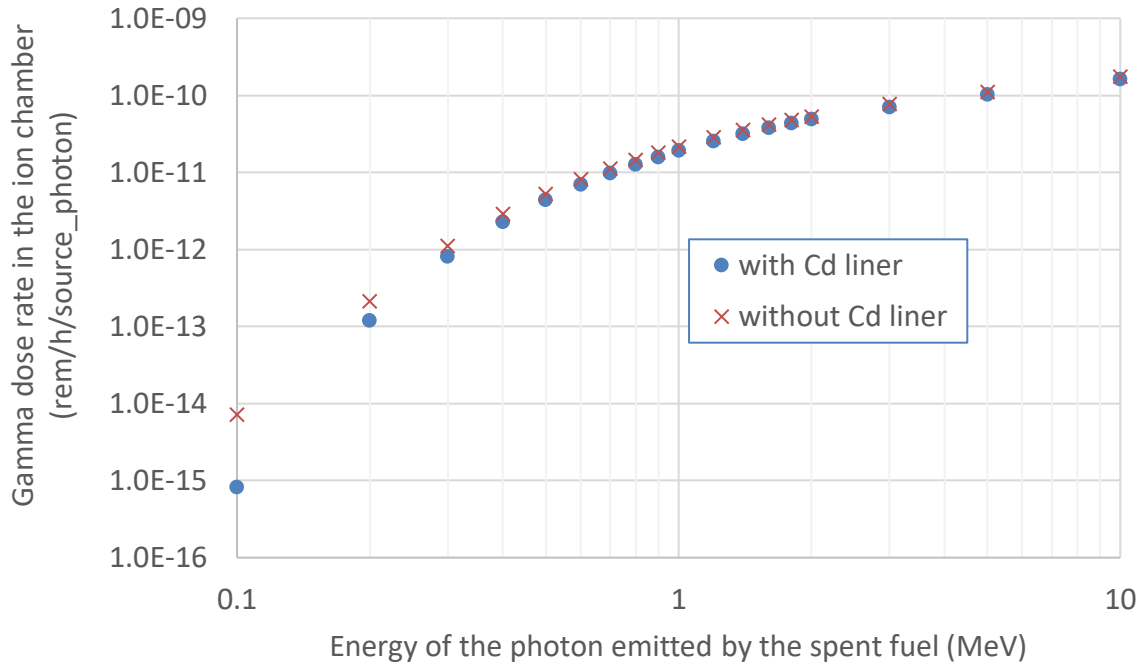

Figure 4. Response functions for the PNAR gamma count rates for the SVEA64 assembly design.

3.2 ORIGEN MODULE FOR ANALYSIS OF PNAR MEASUREMENT DATA

3.2.1 Neutron and Gamma Detector Count Rates

To calculate the neutron and gamma detector count rates from a PNAR measurement, the ORIGEN Module first calls the ORIGEN code to perform the burnup calculations based on operator declarations of the fuel. Then, the passive neutron and gamma emission rates of the fuel calculated by the ORIGEN code are multiplied with the pregenerated MCNP response functions. Neutron emission is usually dominated by ^{244}Cm (and ^{242}Cm at shorter cooling times), which strongly depends on the assembly burnup. Gamma ray emission is generated primarily by fission products and thus also depends on the assembly burnup. Both neutron and gamma count rates can be sensitive to the operating history of the assembly, and previous studies have shown that applying operating history information to the analysis can improve the simulation results. A detailed uncertainty analysis of the neutron and gamma count rate was documented previously [2] and is not repeated herein.

3.2.2 Net Neutron Multiplication

The neutron emissions calculated by ORIGEN includes only the passive neutrons emitted by spontaneous fissions and (α, n) reactions. However, additional neutrons are generated by induced fissions in the fuel, the amount of which depends on the net neutron multiplication (*Mult*) of a given assembly interacting with its surroundings.

To determine the *Mult* for each assembly, the following equation is used:

$$Mult = 1/(1 - k_{eff}) \simeq 1/(1 - k_{\infty}(1 - L)), \quad (1)$$

where k_{eff} and k_{∞} are the effective and infinite neutron multiplication factor, respectively, of the assembly, and L is the neutron leakage factor. ORIGEN calculates k_{∞} as the ratio of total neutron production (fission cross section multiplied by the number of neutrons per fission) over total neutron absorption. There is no geometry associated with this parameter other than the weighting of the neutron cross sections for the assembly design. L is calculated as $L = 1- k_{eff} / k_{\infty}$, where k_{eff} is determined by MCNP for the given fuel assembly geometry and composition.

The leakage factor is largely constant for a fixed PNAR measurement configuration and is only weakly dependent on the fuel composition. L was calculated to be 0.55 and 0.56 for the 8 × 8 and 10 × 10 SVEA assembly designs, respectively. For the remaining three 9 × 9 assemblies, L is assumed to be 0.56. The values stored in the detector response files are the neutron non-leakage probabilities $(1 - L)$. Discussion of uncertainty in L and *Mult* calculations is provided in Section 5.8.

Mult is then used to multiply the raw PNAR neutron count rates calculated by the ORIGEN Module for each assembly to account for the induced fissions in the assembly.

On the PNAR measurement side, *Mult* is not measured directly but is expected to be correlated to the PNAR ratio [7]. As a practical consideration, the measured PNAR Ratio is ~1.04 for a typical discharged assembly [1], indicating a relatively small 4% change in the neutron count rate between the two measurement configurations. Although the ORIGEN simulations could infer the PNAR ratio by using the predicted neutron signals without and with the Cd liner, determination of *Mult* by using Eq. (1) is more direct and eliminates additional uncertainties and complexities associated with simulating the neutron signals under two different multiplying configurations. The multiplication change created by the insertion of the Cd-liner in the current implementation of the PNAR approach is not directly captured in the calculation of *Mult*. The multiplication change is indicated by the measured PNAR ratio, which is expected to trend closely with the predicted *Mult* of the assembly, and this approach was used in this report.

The ORIGEN Module currently does not explicitly output the multiplication of the assembly as part of the standard data exchange interface with IRAP. However, this parameter is calculated and used internally by the software to adjust the calculated neutron count rates to account for induced fissions in the assembly. Software modifications that include multiplication in the exchange data file are being finalized.

3.3 ADDITIONAL CONSIDERATIONS

The LND 52110 ion chamber used in this instrument has a nonlinear response to gamma dose rate [3] as noted previously for Fork detector measurements. Despite the higher bias voltage (500 V instead of the usual 100 V) used in the PNAR measurements, it was determined based on the analysis in this study that these ion chambers still had a nonlinear response. A power function in the form of $y = x^p$ developed in a previous work was used to correct the calculated gamma count rates, where x and y are the calculated count rates before and after the correction. A 0.8 correction factor was applied in the current simulations to account for the nonlinear behavior.

To account for factors (e.g., electronic efficiency) that were not accounted for in the ORIGEN calculations or by the response functions, the averages of the calculated and measured neutron and gamma count rates among the set of 23 BWR fuel assemblies were compared. The ratios of the measured average signals to the calculated averages, referred to as *scaling factors*, were used to scale the calculated neutron and gamma signals for each fuel assembly in the assembly set. Such ratios can be replaced by

calibration factors if sufficient data have been collected by the same PNAR instrument at the same spent fuel pool.

With these adjustments, the calculated singles rates were then compared against the measured ones.

3.4 GRAPHICAL USER INTERFACE (GUI)

There are two ways to perform ORIGEN Module simulations to calculate PNAR or Fork detector count rates and net neutron multiplications: (1) execute the text-based input file through command line, and (2) use the Java-based GUI. The GUI for the ORIGEN Module emulates the function of the module and data exchange with IRAP. A screenshot of the GUI is shown in Figure 5 for an example calculation to calculate the PNAR count rates and net neutron multiplication from a fuel assembly using basic safeguards information for the assembly. The scaling factors discussed in Section 3.3 for neutron and gamma count rates can be entered through this GUI: "ncaa" is for the scaling factor for "neutron-a"; "ncab" is for "neutron-b"; and "gcal" is for gamma. "Neutron-a" is for the total neutron count rates from all four ^{3}He tubes for the "without Cd" case; "neutron-b" denotes those for the "with Cd" case. "Pcoeff" is for the power index discussed in Section 3.3 to account for the ion chamber nonlinear response. "Pnl" is for neutron nonleakage probability (1-*L*). As shown in Figure 5, unity was entered for these scaling factors and for the power index, which means no scaling were performed on the calculated neutron and gamma count rates and no correction was made to the gamma count rate for the nonlinear response in this example. The scalings and correction can be done separately after this ORIGEN Module calculation. No value was entered for "pnl" in this example, which means the default value (0.44) was used for this 9 × 9 assembly. Figure 6 shows part of the ORIGEN Module output file that includes the calculated neutron and gamma count rates for a PNAR measurement. More details of this GUI can be found in the ORIGEN Module manual [10].

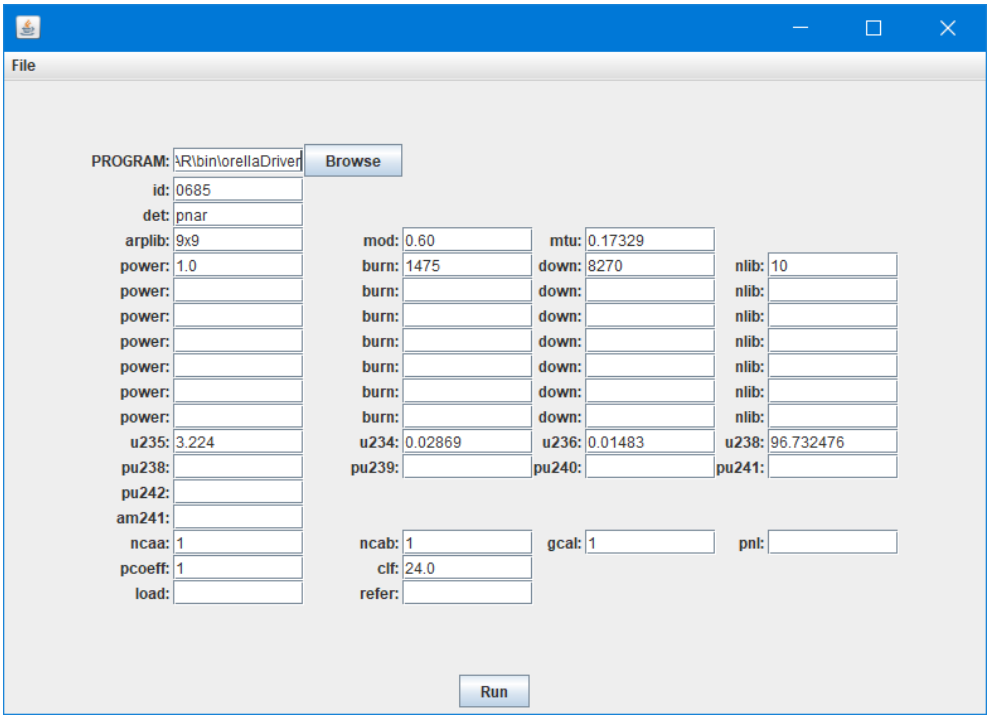

Figure 5. Screenshot of the Java GUI for the ORIGEN Module for an example PNAR measurement analysis.

KIND="gamma";CATEGORY="origen";"COMMENT="2407";NumericResult=13395.5;DateTimeResult="2020-11-04 09:27:04"

KIND="neutron-a";CATEGORY="origen";"COMMENT="2407";NumericResult=226831.5;DateTimeResult="2020-11-04 09:27:04"

KIND="neutron-b";CATEGORY="origen";"COMMENT="2407";NumericResult=210837.1;DateTimeResult="2020-11-04 09:27:04"

Figure 6. Part of the ORIGEN Module output file showing the calculated neutron and gamma count rates for a PNAR measurement.

4. COMPARISON OF CALCULATED AND MEASURED DATA

Calculations were performed with the ORIGEN Module by using safeguards data and operator data as input in the calculations. The results for the PNAR measurements analyses obtained with each of these two datasets are presented in this section.

4.1 ANALYSIS USING SAFEGUARDS DATA

Analyses were performed by using assembly-average initial enrichment, assembly-average burnup, and cooling time from the discharge of the assembly to the measurements. The simulations do not account for detailed assembly design or operational characteristics (e.g., void fraction, burnup) at the height of measurement or the assembly operational history (i.e., days at power per cycle, power for each cycle, or decay time between operating cycles). A simplified irradiation history for each assembly was derived by using the assembly burnup and a representative BWR-specific irradiation power of 24 MW/MTU. The assembly was assumed to operate continuously during this period.

The assembly data provided by STUK for the 23 measured assemblies included assembly type, assembly-average burnup, assembly-average initial enrichment, cooling time, and U and Pu mass in the assembly at discharge from the reactor. The initial U mass in each assembly was inferred by using the ORIGEN burnup code based on the provided information for these assemblies.

ORIGEN Module calculations were performed by using the safeguards data to predict the PNAR neutron and gamma count rates and to estimate *Mult* based on the method discussed in Section 3 for each assembly. A typical BWR core average moderator density (0.4555 g/cm^3) was used in these calculations. Figure 7 shows the relative difference between the PNAR neutron count rate calculated with the ORIGEN Module by using safeguards data and the measured count rate for each of the 23 BWR assemblies. The standard deviation among the 23 assemblies is 11.7% for the neutron count rates without the Cd liner and 11.3% for the neutron count rates with the Cd liner. Sixteen of the 23 assemblies have calculated neutron rates within 10% of the measurement, and the other seven assemblies (BWR1, 2, 5, 23, 31, 35, and 43) have calculation-to-measurement relative differences between -22.9 and 22.4%. BWR1 and BWR2 are two of the three assemblies with noncontinuous cycle histories, as listed in Table 1. Relatively large differences between calculations and measurements are due to the simplification in the used operation history, whereas the local burnup and moderator densities experienced by a BWR assembly at a particular axial node can be significantly different than the assembly-average values included in the safeguards data.

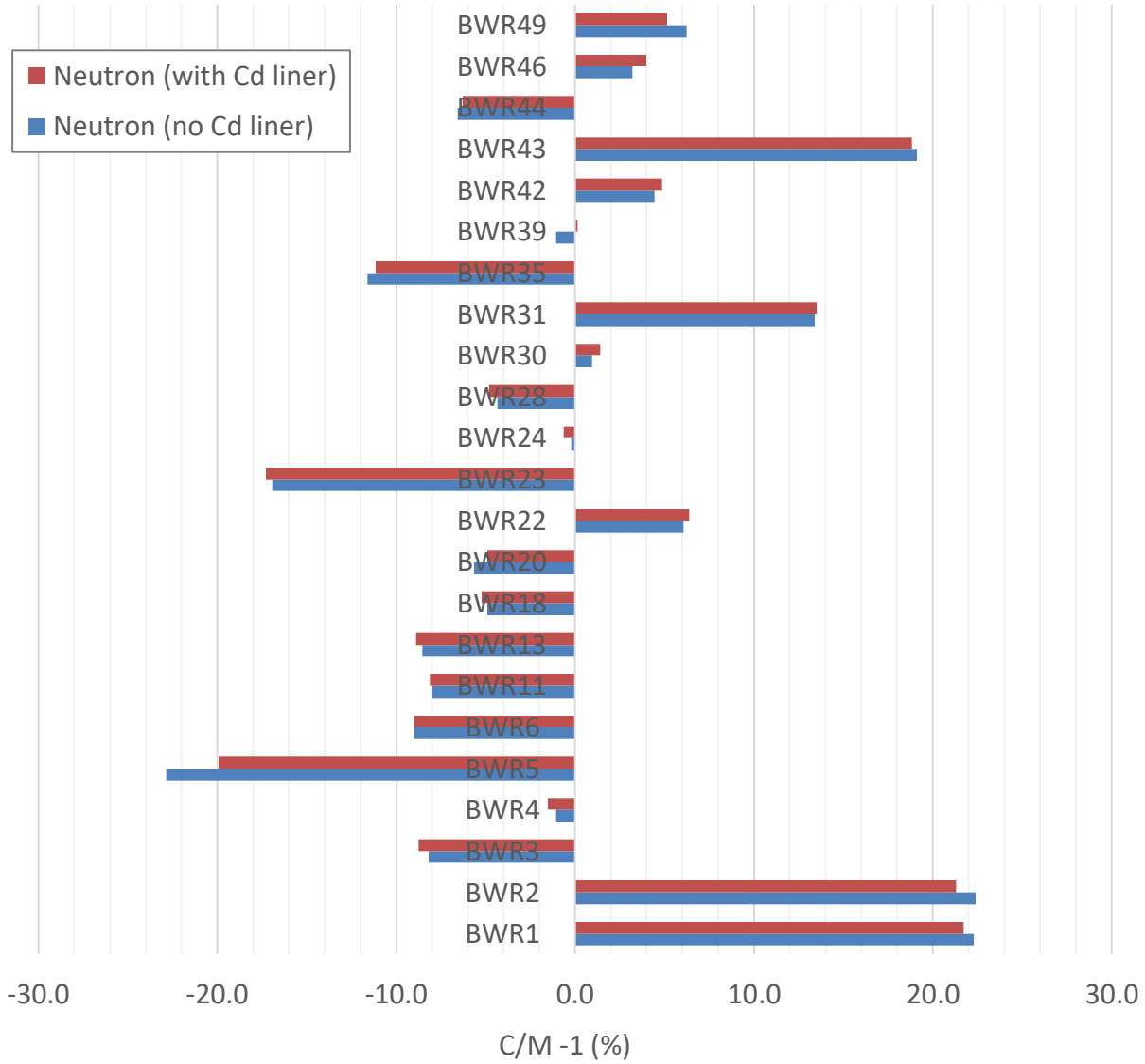

Figure 7. The neutron count rate relative difference between the calculation (C) using safeguards data and PNAR measurement (M) for each assembly.

Figure 8 shows the relative difference between the PNAR gamma count rate calculated with the ORIGEN Module using safeguards data and the measured count rate for each of the 23 BWR assemblies. The standard deviation among the 23 assemblies is 11.8 and 11.9% for the cases with and without the Cd liner, respectively. These differences were 16.3 and 15.4%, respectively, before the correction applied to account for the ion chamber nonlinear response as described previously in Section 3. All assemblies, except for BWR1 and BWR31, had calculated gamma count rates within 16% of the measured values.

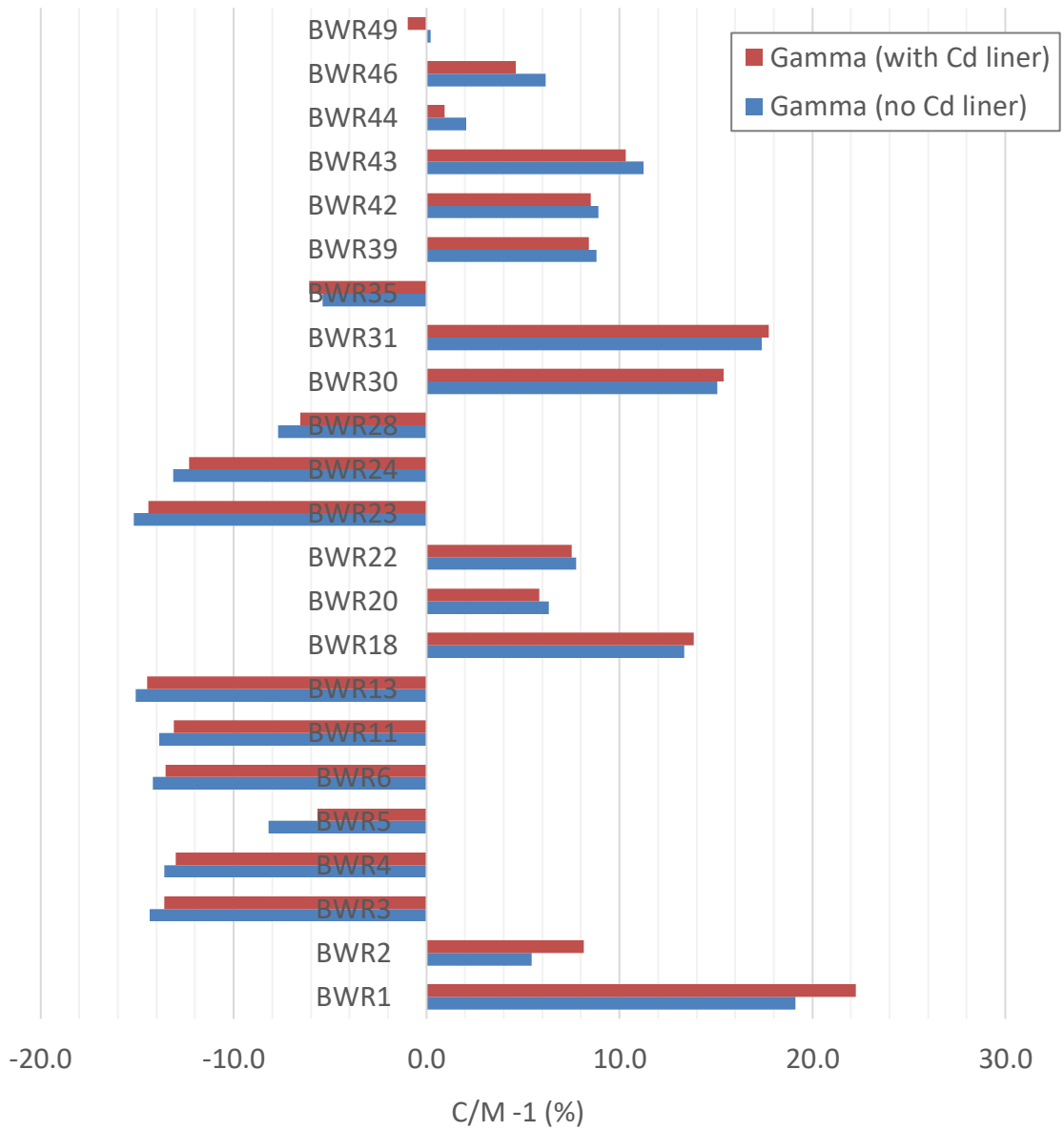

Figure 8. The gamma count rate relative difference between calculation (C) using safeguards data and PNAR measurement (M) for each assembly.

The observed calculation-to-measurement differences for neutron and gamma count rates are similar to those observed in the ORIGEN Module analysis of Fork detector measurements for BWR assemblies [3] and are mainly due to the complexities in BWR fuel design and operating conditions.

Figure 9 compares the calculated *Mult* with the measured PNAR ratio. The error bars (horizontal direction) on the measured PNAR ratios include the statistical uncertainty listed in Table 1 and a repeatability uncertainty of 0.0013. The error bars for calculations are estimated as a sum of 2.7% uncertainty due to the variability in the assembly-to-assembly burnup profile at the measurement position and enrichment variability at the measurement position to that of the assembly-average, and a 2%

uncertainty associated with the calculation of *Mult*. No uncertainty has been assigned for cooling time or U mass. A detailed uncertainty analysis is included in Section 5.

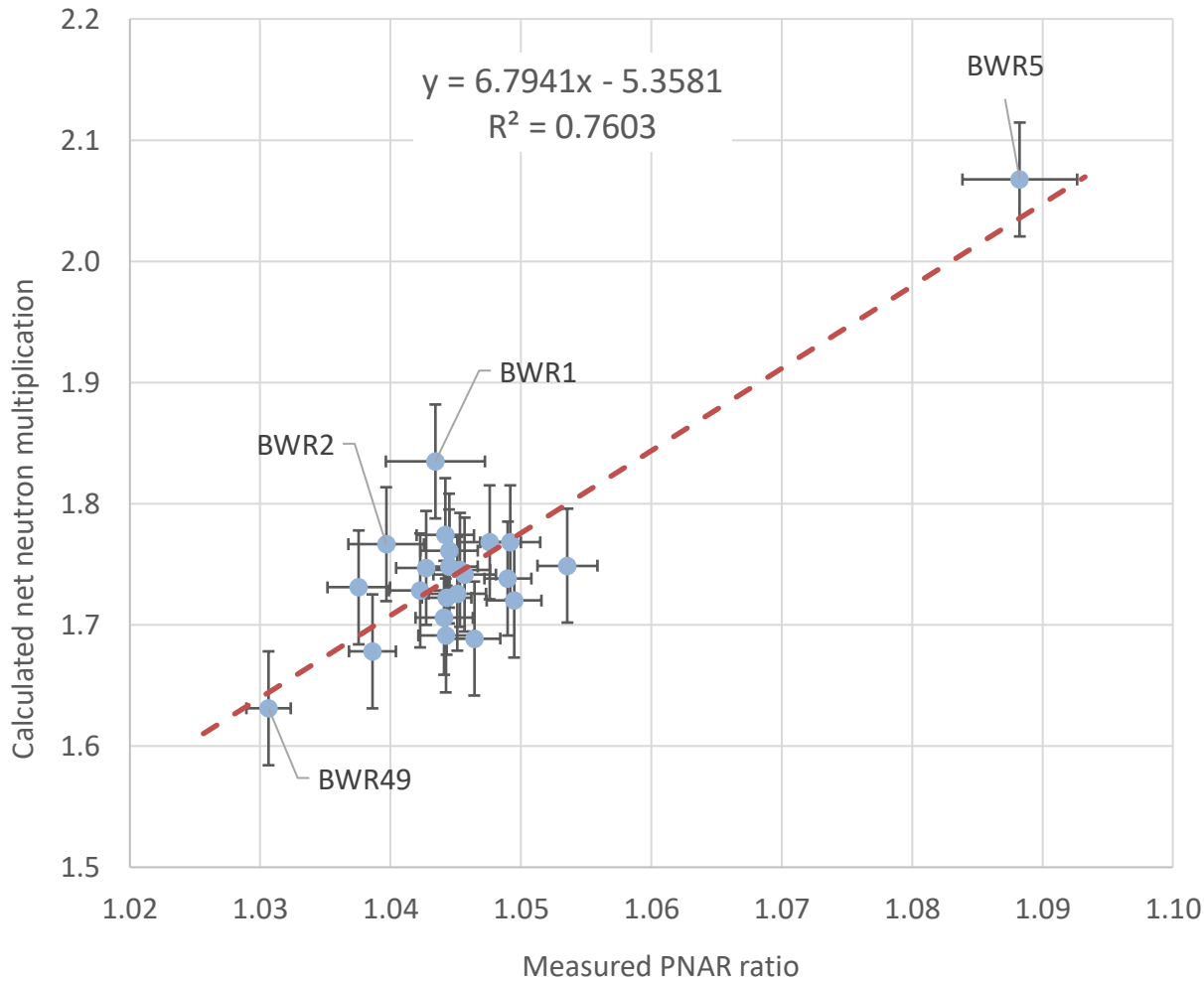

Figure 9. Calculated net neutron multiplication using safeguards data vs. measured PNAR ratio. The linear fit equation and the goodness of fit parameter (R^2) is also shown.

For assemblies with axial enrichment zoning, the enrichment at the midsection of the assembly is on average 6% greater than the assembly-average and is expected to exhibit as a systematic bias of 1.8% in *Mult* compared with assemblies without axial enrichment zoning. As expected from a physics standpoint, a clear difference is seen in Figure 9 for the highest multiplying assembly, BWR5, and lowest assembly, BWR49, compared with the remainder of the assemblies. BWR1 exhibits one of the largest deviations from the trendline. This assembly was operated in non-contiguous cycles and was also an initial core assembly. In previous studies that used the Fork detector [3], first cycle assemblies exhibited a systematic bias compared with other assemblies. This might be caused by unusual reactor operation during the commissioning phase of start-up, the unique assembly design features, or reactivity control mechanisms that are not captured in the simulations. Most other assemblies fall within a narrow envelope that is representative of the reactivity (multiplication) of typical discharged fuel.

Table 3 lists the calculated neutron and gamma count rates (after making the adjustments described in Section 3) and *Mult* for all 23 assemblies. The uncertainty for *Mult* is estimated as the relative difference between the calculated *Mult* and the expected value according to the linear trend line in Figure 9. The

estimated uncertainty in measurements and simulations is consistent with the observed deviations in the data from the trend line. The relative standard deviation of the results is 2.25%. Assemblies with part-length rods or axial enrichment zoning do not appear to have any consistent biases compared with other assemblies. The largest deviations are observed for the 8 × 8-1 and 9 × 9-1AB assembly designs.

Table 3. Calculated neutron count rates, gamma count rates, and *Mult* using the ORIGEN Module with safeguards data.

Assembly #	Assembly type	Without Cd liner		With Cd liner		*Mult*	%Differences in *Mult**
		Neutron, cps	Gamma, cps	Neutron, cps	Gamma, cps		
1	8 × 8-1	857.8	110,457.0	818.2	94,935.2	1.835	5.99
2	8 × 8-1	3,903.5	185,821.7	3,721.1	159,742.6	1.767	3.59
3	SVEA-64	7,139.2	239,247.7	6,804.7	205,741.9	1.747	1.20
4	SVEA-64	10,711.8	258,100.1	10,209.3	221,967.3	1.691	-2.60
5	SVEA-64	748.3	149,959.0	713.7	128,899.1	2.068	1.56
6	SVEA-64	6,547.5	239,382.0	6,240.8	205,863.0	1.768	-0.11
11	SVEA-64	6,226.0	234,106.8	5,934.3	201,312.0	1.768	0.50
13	SVEA-64	8,525.5	249,276.4	8,125.8	214,372.9	1.726	-0.97
18	9 × 9-1AB	6,038.0	279,652.4	5,800.0	238,706.2	1.731	2.35
20	ATRIUM10	9,670.4	332,669.5	9,288.4	284,119.4	1.720	-2.94
22	SVEA-100	9,271.7	323,871.9	8,905.6	276,541.8	1.706	-1.72
23	SVEA-64	7,075.8	238,870.6	6,744.2	205,417.3	1.748	0.58
24	SVEA-64	6,459.8	234,899.5	6,157.2	201,999.1	1.761	1.33
28	SVEA-64	5,960.1	231,934.3	5,680.9	199,447.7	1.774	2.18
30	9 × 9-1AB	6,306.8	291,374.8	6,058.1	248,739.5	1.742	-0.28
31	9 × 9-1AB	6,898.1	295,620.5	6,626.0	252,368.4	1.728	0.30
35	SVEA-96	13,874.2	372,864.5	13,325.5	318,547.7	1.689	-3.57
39	ATRIUM10	7,714.0	318,751.0	7,409.5	272,217.2	1.749	-2.84
42	GE12	9,160.3	331,691.4	8,798.6	283,276.8	1.745	0.08
43	GE12	21,978.2	447,074.2	21,108.3	382,133.3	1.678	-1.19
44	GE14	19,430.3	481,721.9	18,661.4	411,876.3	1.722	-0.84
46	GE14	24,729.8	694,244.6	23,750.6	594,209.2	1.738	-1.74
49	ATRIUM10	32,041.3	493,199.4	30,772.4	421,636.7	1.631	-0.79
						Relative standard deviation	2.25

*The relative difference between the calculated *Mult* and the value obtained from the linear trendline in Figure 9.

Additional analyses were performed by using the average operating conditions at axial node 8 of a representative assembly with the ORIGEN Module calculations. The results obtained are similar with the ones presented herein because using the average values of node 8 does not account for the variations from one assembly to another.

4.2 ANALYSIS USING OPERATOR DATA

Node-by-node burnup and moderator densities for all 23 assemblies were extracted from the CASMO/SIMULATE SNF output files provided by the reactor operator, TVO. Burnup values and

moderator densities of node 8 from the operator data were used in the ORIGEN calculations—in addition to initial Uranium loading, initial enrichment, and cooling time—to reflect the assembly characteristics in proximity to the axial measurement position of the assembly. The node-by-node data are not provided in a typical safeguards dataset. The ORIGEN Module simulations assumed a continuous cycle history and a constant specific irradiation power of 24 MW/MTU, which is a representative power level for BWR assemblies.

Figure 10 shows the relative difference between the PNAR neutron count rate calculated with the ORIGEN Module using operator data and the measured count rate for each of the 23 BWR assemblies. Compared with the neutron count rates obtained by using safeguards data (Figure 7), the results were significantly improved when using operator data. The standard deviation among the 23 assemblies is 3.9 and 4.4% for the neutron count rates with and without the Cd liner, respectively. These values are almost three times lower compared with those corresponding cases when safeguards data were used (11.3 and 11.7%, respectively). All assemblies' calculated neutron count rates are within 10% of the measurements, with 18 assemblies showing differences in the calculation-to-measurement of less than 5%.

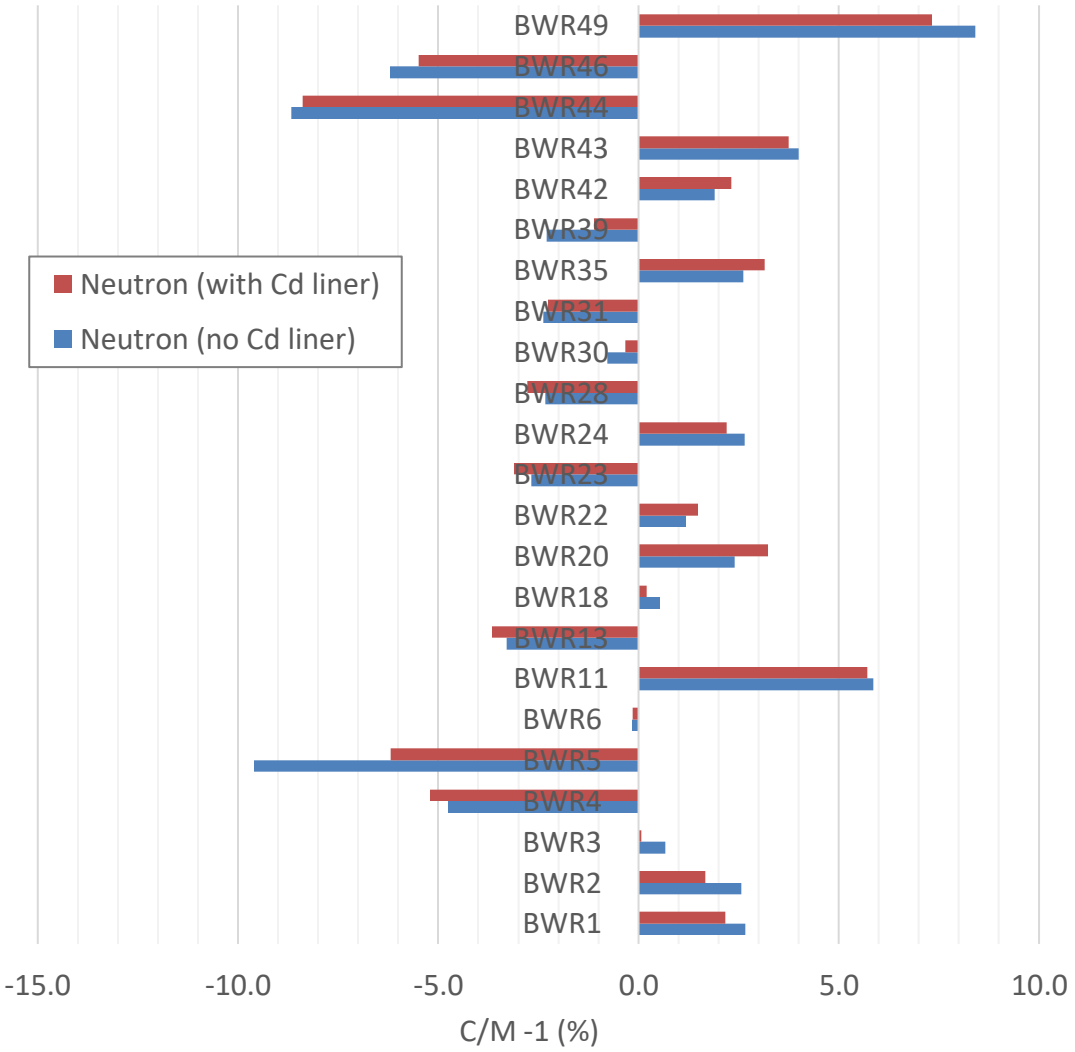

Figure 10. The relative differences between the calculated (C) PNAR neutron count rates using operator data and the measured (M) values for each assembly.

Figure 11 shows the relative difference between the PNAR gamma count rate calculated with the ORIGEN Module by using operator data and the measured count rate for each of the 23 BWR assemblies. The standard deviation among the 23 assemblies is 10.9 and 11.0% for the cases with and without the Cd liner, respectively. All assemblies—except for BWR1, BWR13, and BWR30—show calculated rates that are within 15% from the measured values. The gamma count rate results are only marginally improved compared with the cases when safeguards data are used.

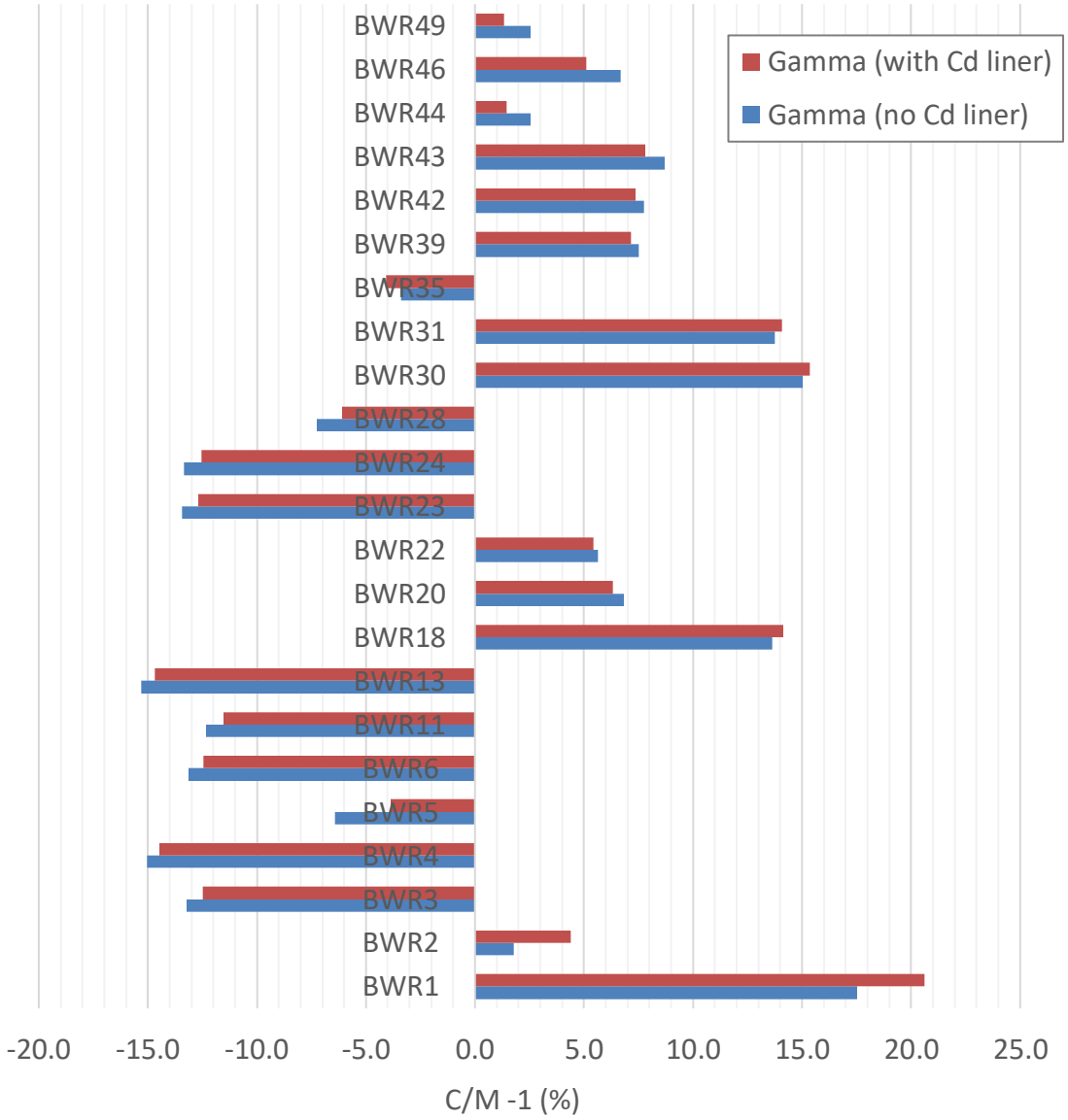

Figure 11. The relative difference between the calculated (C) PNAR gamma count rates using operator data and the measured (M) values for each assembly.

Figure 12 compares the calculated *Mult* with the measured PNAR ratio. The error bars (vertical direction) of 2.3% on the calculated values are based on the estimated uncertainty in the TVO node burnup value of 3% and an added 2% associated with the multiplication calculation. A detailed uncertainty analysis is

included in Section 5. The results are generally very similar to those obtained with only safeguards data (i.e., assembly-average characteristics), as shown in Figure 9. A comparison of assembly multiplication values with and without operator information shows that *Mult* decreases by using the operator data for the measurement position compared with the assembly-average data by a relatively consistent factor of 0.96 ± 0.01 for all assemblies. The reduction is driven primarily by the increased burnup at the measurement position, which is better captured in the operation data.

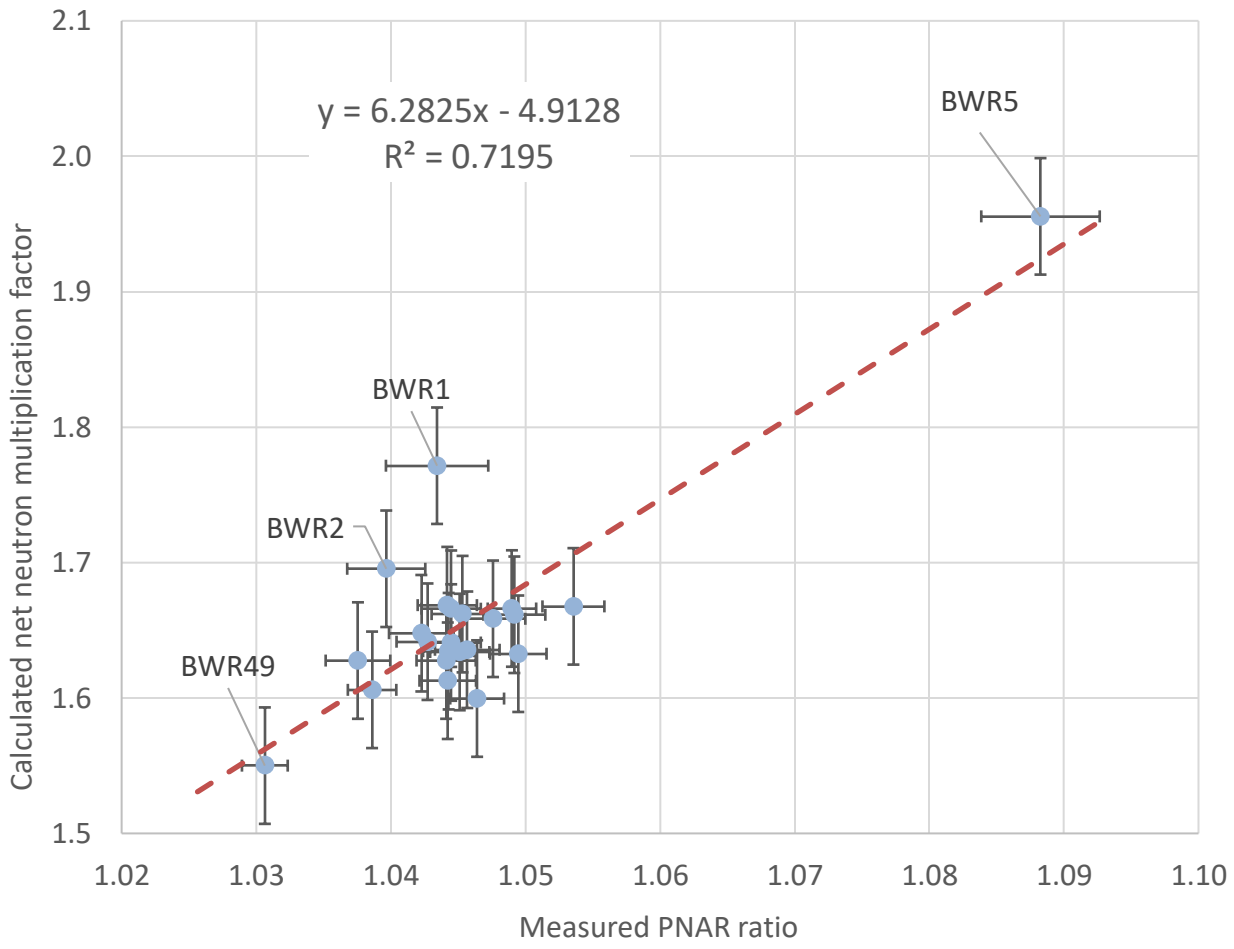

Figure 12. Calculated net neutron multiplication using operator data vs. measured PNAR ratio. The linear fit equation and the goodness of fit parameter (R^2) is also shown.

Additional calculations were performed by using the cycle dates and power history information in addition to the operator data used here to assess the relative importance of operating history information. In these calculations, the node-specific enrichment and burnup were used. Assembly *Mult* values were relatively unaffected with changes of < 0.5%. The low importance of operating information on assembly *Mult* is unsurprising since the primary fissile materials including U and Pu isotopes depend mainly on the final burnup. Only ^{241}Pu, with a half-life of 14 years, will show any significant dependence on operating history information. The neutron count rates are also relatively unaffected by neglecting the history information. The gamma results are marginally improved with the standard deviation reduced from 11 to 9.2%, which is likely because only three of the 23 assemblies had noncontinuous cycle history. These findings indicate that using a continuous cycle history is a reasonable assumption for this specific set of assemblies, although much larger differences were found in our previous work [3].

Table 4 lists the calculated results of neutron and gamma count rates (after making the adjustments described in Section 3) by using operator data and the *Mult* for all 23 assemblies. The *Mult* uncertainty is estimated as the relative difference between the calculated value with the ORIGEN Module and the expected value according to the linear trend line shown in Figure 12. The estimated uncertainty in measurements and simulations is consistent with the observed deviations in the data from the trend line. The relative standard deviation of the results is 2.44%. The largest deviations are observed with the 8 × 8-1 and 9 × 9-1AB assemblies. A review of other assembly designs (e.g., lattice type, part-length rods, axial enrichment zoning) did not show any clear design-related systematic bias.

Table 4. Calculated neutron count rates, gamma count rates, and *Mult* using the ORIGEN Module with the operator data.

Assembly #	Assembly type	Without Cd liner		With Cd liner		*Mult*	%Differences in *Mult**
		Neutron (cps)	Gamma (cps)	Neutron (cps)	Gamma (cps)		
1	8 × 8-1	720.1	108,978.2	686.7	93,661.4	1.772	7.85
2	8 × 8-1	3,271.7	179,365.0	3,119.0	154,189.7	1.695	4.73
3	SVEA-64	7,829.0	242,402.0	7,462.8	208,451.8	1.642	0.21
4	SVEA-64	10,309.7	253,768.9	9,827.2	218,240.0	1.613	-2.11
5	SVEA-64	876.8	152,829.9	836.2	131,374.5	1.956	1.63
6	SVEA-64	7,183.4	242,317.9	6,847.4	208,386.2	1.661	-1.02
11	SVEA-64	7,163.2	238,321.8	6,828.1	204,941.4	1.658	-0.61
13	SVEA-64	9,015.9	248,668.4	8,594.0	213,849.6	1.634	-1.16
18	9 × 9-1AB	6,382.8	280,373.6	6,131.5	239,321.6	1.628	1.37
20	ATRIUM10	10,496.3	334,227.6	10,082.7	285,464.1	1.633	-2.84
22	SVEA-100	8,843.2	317,581.8	8,494.9	271,169.2	1.628	-1.16
23	SVEA-64	8,289.0	243,764.4	7,901.1	209,629.6	1.641	-0.50
24	SVEA-64	6,644.5	234,327.2	6,333.8	201,507.9	1.666	1.02
28	SVEA-64	6,085.3	232,999.3	5800.8	200,355.2	1.669	1.29
30	9 × 9-1AB	6,198.3	291,254.0	5,954.3	248,625.4	1.636	-1.27
31	9 × 9-1AB	5,939.1	286,436.9	5,705.3	244,514.2	1.648	0.77
35	SVEA-96 Optima	16,105.3	380,766.3	15,470.0	325,322.9	1.600	-3.71
39	ATRIUM10	7,618.0	315,017.0	7,318.0	269,031.7	1.668	-2.26
42	GE12	8,937.6	328,122.1	8,585.5	280,230.5	1.662	0.45
43	GE12	19,189.5	436,913.9	18,432.4	373,419.1	1.606	-0.39
44	GE14	18,992.8	484,178.4	18,243.5	413,971.1	1.635	-0.81
46	GE14	22,474.6	697,436.8	21,587.8	596,948.6	1.666	-0.68
49	ATRIUM10	32,702.2	504,739.9	31,411.4	431,465.0	1.550	-0.78
						Relative standard deviation	2.44

*The relative difference between the calculated *Mult* and the value obtained from the linear trendline in Figure 12.

5. UNCERTAINTY ANALYSIS

Uncertainties in the input data used in the ORIGEN Module calculations will result in deviations between predicted and measured observables. An analysis of these uncertainties was performed to identify and quantify the primary sources of uncertainty in the calculations.

The calculations use the following input data:

- Uranium (U) mass (of the assembly);
- initial enrichment (at the measurement height vs. assembly average);
- burnup;
- moderator density;
- operating history of the assembly (including the operating days, the specific power, and the time between cycles for each cycle), if available; and
- cooling time.

The potential uncertainty in the calculated signals was estimated by perturbing each input parameter independently by an amount estimated to be representative for these analyses. Assuming first-order sensitivities, the impact of larger or smaller uncertainties can be estimated. The assembly used in these uncertainty calculations was a representative measured assembly (BWR24) with an 8 × 8 assembly lattice and a SVEA64 design. The results are summarized in Table 5.

Table 5. Uncertainty analysis of predicted observables due to modeling uncertainty.

Model input parameter	Parameter Uncertainty (%)	Predicted uncertainty in observables		
		Gamma (%)	Neutron (%)	Multiplication (%)
U mass	5	5	5	0
^{235}U initial enrichment	6	< 0.03	-10.9	1.8
Burnup	5	5.1	23.0	-1.8
Moderator density	10	-0.1	-5.3	< 0.02
Cooling time	5	-2.7	-3.8	-0.2

An analysis of assembly history data was performed by using TVO operating data for the fuel characteristics with and without the detailed operating history data. These uncertainty calculations are described separately in Section 5.7.

Each input parameter is discussed in the context of uncertainties in modeling the BWR assemblies. The discussion focuses on multiplication, but the impact of uncertainties on all observables is provided in Table 5.

5.1 ISOTOPE CONCENTRATIONS

To assess the accuracy of the ORIGEN burnup calculations, the ORIGEN-predicted nuclide concentrations for the major actinides of U and Pu were first compared with the values predicted by using the Studsvik code SNF, as provided by TVO. This comparison provides an independent verification of the results, although no measurements are involved. The SNF calculated values are assumed to be more accurate than the ORIGEN calculated values since the SNF calculations use the detailed design and

operating information from CASMO and SIMULATE, which were not applied in the ORIGEN calculations.

The ORIGEN Module calculations were performed by using only basic safeguards information on each assembly. The calculations used the assembly-average enrichment and burnup. The moderator density was assigned a value of 0.4555 g/cm^3, which was the average value for all measured assemblies.

The results for ^{235}U, ^{239}Pu, and total Pu are shown in Figure 13 for all measured assemblies. These three quantities characterize the primary fissile isotopes in the spent fuel assemblies. The ^{235}U content exhibits a consistent bias (i.e., underprediction) of ~15% relative to SNF with a standard deviation of 6%. The ^{239}Pu content has a bias of 3% and a standard deviation of 8%. The total Pu is predicted with an average bias of less than 1% and standard deviation of 5%. The ^{235}U results exhibit larger deviations in this study compared with spent fuel measurements [11], where ^{235}U was overpredicted by ~4% on average compared with measurements; however, the present calculations do not apply any detailed design or operating history information of the assemblies.

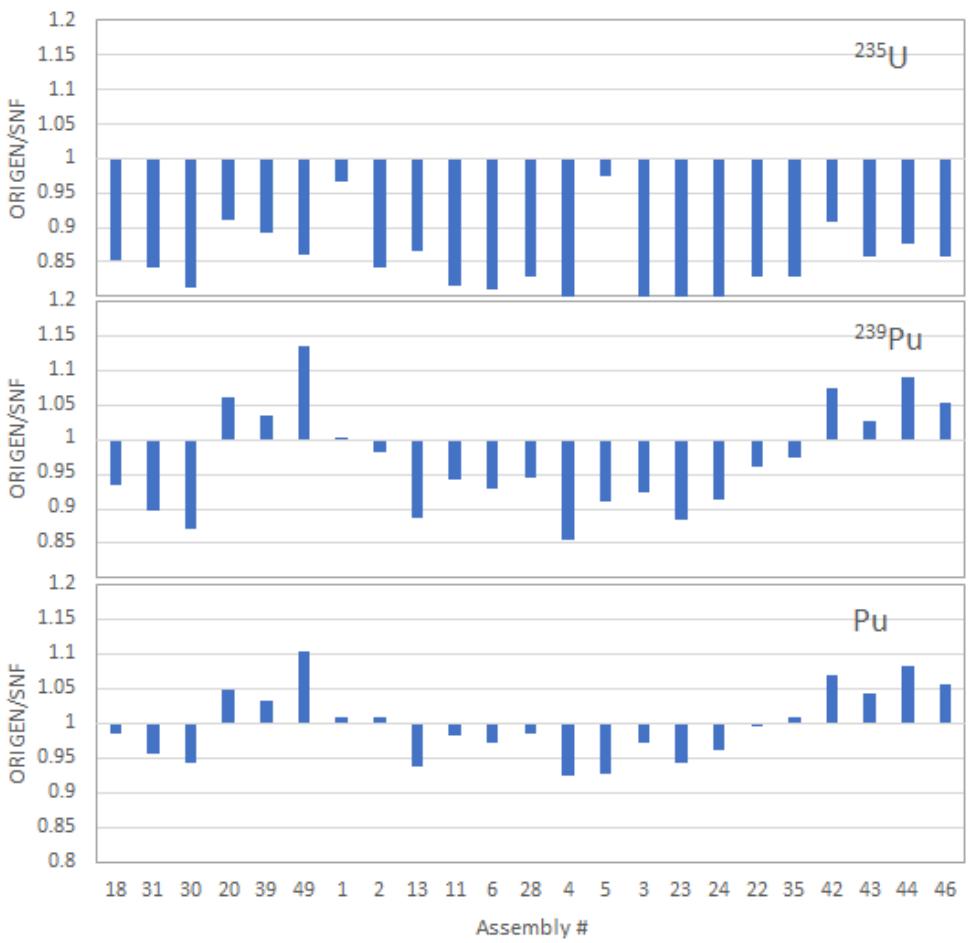

Figure 13. Comparison of nuclide contents predicted by ORIGEN and the SNF code for all measured assemblies. Values for each assembly are shown as the ratio of the ORIGEN over the SNF nuclide/element mass.

5.2 ASSEMBLY URANIUM MASS

The initial U mass is used in the calculations to account for relative differences in U for different assemblies and assembly designs. This mass usually has a very small uncertainty. In the calculations, the U mass (linear) in the vicinity of the detectors influences the measured signals. For assemblies with part-length rods, the linear U mass in the lower region (i.e., dominant zone) is greater than for the upper region (i.e., vanished zone). Therefore, the assembly linear U mass depends on the axial height of the measurements.

For measurements performed in the dominant zone, the linear U mass is typically 3–5% greater than the assembly-average linear mass, depending on the number of partial length rods and the length of the vanished zone. Therefore, the initial U mass for assemblies with part-length rods should be increased when measurements are performed in the dominant zone.

The relationship between U (linear) mass and neutron/gamma count rates is linear (Table 5), as expected. Therefore, assemblies with part-length rods are expected to be underpredicted 3–5% relative to other assemblies if the assembly mass is not adjusted. The U mass only impacts the neutron and gamma detector count rates, not the calculated multiplication factor, which is determined by using a leakage factor that is calculated for the dominant region of the assembly.

5.3 INITIAL ^{235}U ENRICHMENT

The assembly-average initial ^{235}U enrichment is provided in the safeguards declaration record and is generally well-known. However, modern BWR assembly designs can use different axial enrichments in the enriched zone and have natural U blankets in the top and bottom of the fuel rods. Consequently, the ^{235}U enrichment at the height of measurement might be greater than the assembly-average enrichment.

The enrichment of each assembly axial node was available from the information provided by TVO. For the measured assemblies with axial enrichment zones, the enrichment at the measurement height (node 8) was 4–7% greater than the assembly-average enrichment. The average difference for all assemblies was 6%. The potential bias introduced in the calculated multiplication (Table 5) is 1.8%.

5.4 BURNUP

The assembly burnup is part of the operator declaration and can be obtained from the core simulations. Estimates of the accuracy of the predicted assembly burnup are typically ~2–3%, although it might increase for assemblies in regions near the core periphery.

The axial burnup profile of the assembly results in larger burnup values at the measurement position compared with the average. Axial burnup data were provided by TVO for the measured assemblies. The burnup at the height of the PNAR measurements (node 8) was 13–22% greater than the average burnup of the assembly with a mean difference of 18%. The potential bias in the calculated observables introduced by using the assembly-average burnup instead of burnup at the measurement position is significant. By scaling the results in Table 5, an 18% increase in burnup will introduce a ~7% decrease in multiplication. Larger biases are introduced in the neutron and gamma count rates. The effect of this burnup-caused bias is mitigated to a great extent in the data analysis procedure since all assemblies have a larger burnup at the measurement position, and all assemblies will have a similar bias in calculated multiplication. The impact will be noted, especially between assemblies that have different axial burnup profiles.

The axial burnup profiles of all measured assemblies are illustrated in Figure 14. All profiles are normalized to unity. The profiles show that at the measurement position (node 8), the ratio of the node to

average burnup has a relatively low variability between different assemblies. The mean ratio is 1.18 with a relative standard deviation of less than 2.3%. This suggests that uncertainty in multiplication due to a 2.3% variability in burnup at the measurement position for different assemblies is ~1%. Lower burnup variability is observed in nodes 10–12, which have a standard deviation of ~1.5%.

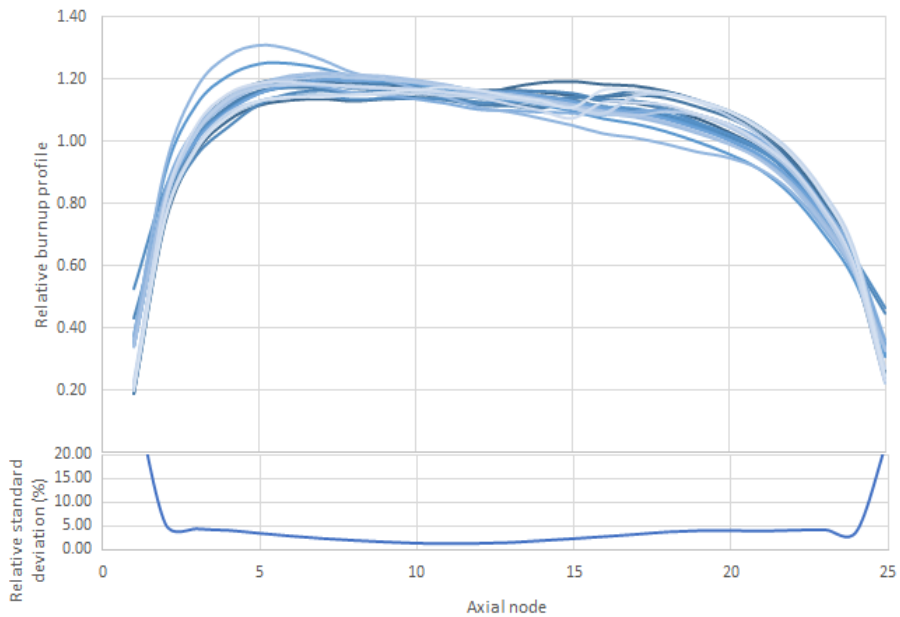

Figure 14. Normalized burnup profiles of all measured assemblies (top) and relative standard deviation of the burnup (bottom) in each of the 25 axial nodes. Nodal burnup data were provided by TVO.

Another observation is that for assemblies with enrichment zoning, the enrichment at the measurement position is larger than the average (i.e., both enrichment and burnup are increased). Since the effects of these increases are anticorrelated (Table 5), this tends to reduce the bias somewhat. For assemblies without axial enrichment zoning, the bias is expected to be larger relative to assemblies with zoning.

These observations are based on the 23 measured assemblies, and the study of more assemblies might be warranted to confirm these findings. The burnup profile could be obtained by an axial gamma ray scan of the assembly if this information is not available from the operator.

5.5 MODERATOR DENSITY

The density of the moderator (i.e., water) for a BWR assembly varies drastically along the vertical axis of the assembly, and the axial profile also varies occasionally due to several factors, including the power variation of the assembly. The moderator density is usually ~0.76 g/cm^3 at the inlet, and it can vary from 0.17 to 0.28 g/cm^3 at the outlet. The moderator density is often indicated by means of void fraction, which is almost inversely proportional to moderator density. Moderator density strongly influences the actinides build-up, including Pu and Cm (i.e., main neutron emitter), during irradiation and thus on neutron multiplication factor and neutron emission rates in the spent fuel assembly. If this parameter is not available from the operator, then an assembly-average moderator density of 0.45 g/cm^3 is sometimes assumed. Depending on where the PNAR measurement is taken along the height of the assembly, the moderator density on that height might be larger or smaller than the assembly-average value.

Several studies have estimated that the error in the moderator density calculated by thermal hydraulics codes is ~5–6%. For the measured assemblies, the assembly-average water moderator density is 0.45

g/cm^3 ± 8%. The average density in node 8 is 0.56 g/cm^3 ± 8%, approximately 24% larger than the assembly-average value. Assuming that an average moderator density is available for the measurement height, a conservative uncertainty due to an assembly variation of 10% is estimated. The potential uncertainty in multiplication due to moderator density uncertainty is <0.03%.

5.6 COOLING TIME

The cooling time of the assembly is part of the operator declaration and is assumed to be well-known. For a nominal error of 5% in the cooling time (~1 year for many of the measured assemblies), the bias in the calculated multiplication (Table 5) is ~0.2%. Larger biases are observed in the neutron and gamma count rates. Generally, the error in cooling time is not expected to be significant.

5.7 OPERATING HISTORY

Operating history, as used in this report, includes the irradiation days (i.e., cycles dates), the time between cycles (i.e., downtime and any extended decay time if the assembly was removed from the core and reinserted at later dates), and the assembly power for each irradiation cycle. This information was provided by TVO for all assemblies. When information is unavailable, continuous irradiation is usually modeled by using the date of first charge and the date of final discharge or by using a constant irradiation power with an inferred total irradiation time based on the final burnup.

The impact of history information was evaluated for the measured assemblies. For assemblies that operated during contiguous cycles in the reactor (i.e., were not removed from the core and reinserted in a later cycle), the impact of having assembly-specific operating history is expected to be minor. Three assemblies were irradiated in noncontiguous cycles. These were analyzed separately because the impact of history data is expected to be larger.

5.8 NET NEUTRON MULTIPLICATION

The methodology used to calculate the *Mult* and how it is used to correct the calculated neutron count rates are described in Section 3. *Mult* is influenced by the neutron leakage factor (L), a parameter calculated for the assembly design by using MCNP. This parameter and the assumptions in its development and application contribute to uncertainties in the simulations and are discussed in this section.

An uncertainty of 1% in *Mult* might result from having only two digits of accuracy on the values of ($1 - L$), and another ~2% uncertainty might result from assigning the L value of the 10 × 10 assembly design to the 9 × 9 design. Further improvements might be realized by developing explicit leakage factors for other assembly designs.

The approach considers L values to depend only on the assembly design. This is approximate since the leakage factor exhibits some variation, depending on the enrichment and burnup of the fuel. A comparison of *Mult* as calculated by the ORIGEN Module with constant L and *Mult* calculated by using MCNP with the same fuel compositions is illustrated in Figure 15. Although the values trend closely, ORIGEN underpredicted *Mult* for low-burnup fuel and overpredicted *Mult* for high-burnup fuel relative to the MCNP values.

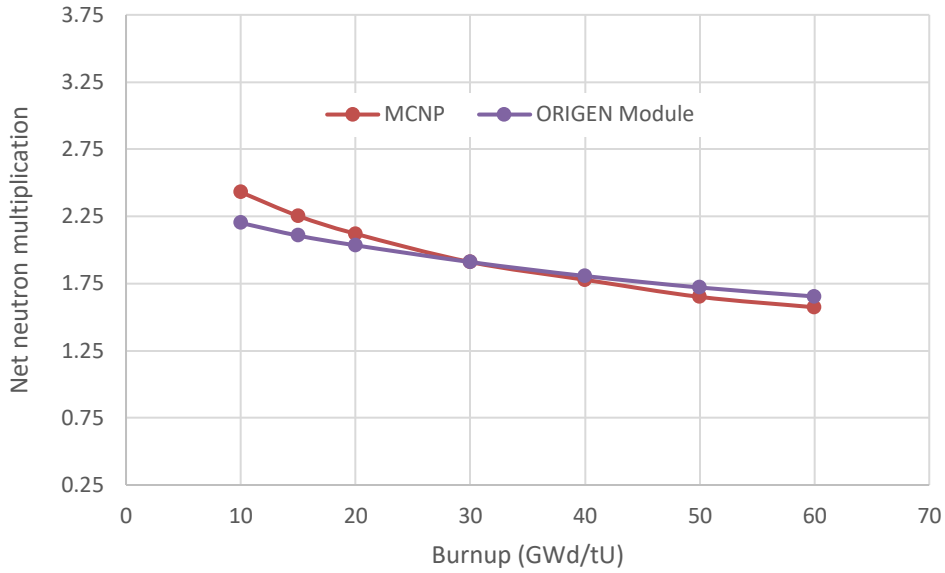

Figure 15. Assembly net neutron multiplication calculated by using the ORIGEN Module and MCNP.

For the case of the highest multiplying assembly BWR5, the burnup was about half the typical discharge burnup for an assembly with an initial enrichment of ~1.9%. Figure 15 suggests an error of ~4% in the calculated neutron multiplication compared with that from the detailed MCNP analysis.

The discrepancy in calculated *Mult* between ORIGEN and MCNP is likely caused by an increase in *L* due to spectral hardening in high-burnup fuel, resulting from the greater accumulation of fission products, which is not accounted for in the ORIGEN calculations. A separate analysis of BWR assemblies performed for burnup credit studies [12] indicates that the average energy of fission (i.e., spectral hardening) increases with increasing burnup, which is consistent with increased neutron leakage.

Improvements by the ORIGEN Module in the calculated *Mult* could be realized by accounting for the change in neutron spectrum with burnup in the calculations for *L*. Although ORIGEN does not perform a neutron transport calculation, information on the spectrum is available through the cross sections used in the burnup analysis, which are derived by using a neutron transport calculation.

However, it is not obvious that accurately reproducing the MCNP-calculated values of *Mult* is required in the context of PNAR ratio data analysis. What is required is that relative differences in *Mult* associated with enrichment, burnup, and assembly design can be predicted accurately. At this time, the potential benefits from improved leakage factor estimation have not been investigated.

6. CONCLUSIONS AND RECOMMENDATIONS

The PNAR instrument is designed to measure the neutron multiplication of a fuel assembly to ensure that it is multiplying at a level consistent with the declaration and the expected fissionable material content in the assembly. The instrument also measures neutron and gamma count rates like those acquired by the Fork detector.

This report documents the analysis of the PNAR system measurement signals by using the ORIGEN Data Analysis Module. The module was originally developed for the Fork detector measurement of spent fuel, and it was expanded for PNAR analysis in this study by generating new response functions specific to the PNAR measurements. The analyzed PNAR measurements were performed in Finland for 23 BWR spent fuel assemblies. When typical safeguards data were used in the ORIGEN Module calculations, the standard deviations between measured and simulated neutron and gamma detector count rates were similar to the results seen in earlier studies that used the Fork detector. The agreement between the calculated count rates and the measurement values was improved by using detailed design and operating information, especially for burnup and moderator density, compared with the case when typical safeguards data that are assembly-average characteristics are used in the simulation. Using detailed operator data resulted in a standard deviation of the calculated-to-measured value among the 23-assembly set of ~4% for neutron and 10% for gamma count rates.

The measured PNAR ratio was analyzed by trending the PNAR ratio with the calculated net neutron multiplication of the assembly since a relationship between measured PNAR ratio and net neutron multiplication has not yet been established. The results show a clear trend between the measured PNAR ratio and calculated net neutron multiplication based on the declaration information. The relative standard deviation between the calculated net neutron multiplication and the values obtained from a linear regression fit of the data is ~2.25%, assuming that all error is attributed to the simulations. The deviations of the data with the linear relationship are consistent with the estimated uncertainties in the simulations.

The PNAR ratio results are only slightly improved when using operator data compared with the case when only assembly safeguards declaration information is used. Simulated assembly net neutron multiplication decreases by ~4% when using operator data for the measured assembly node, due to increased burnup at the measurement position compared with the assembly-average burnup and an increase in enrichment for axial-zoned enrichment. The variability for net neutron multiplication is very similar for simulations performed with and without operator data.

Assemblies without axial enrichment zoning are expected to exhibit a bias relative to zoned assemblies when using only safeguards data, since the enrichment at the measurement position is equal to that of the assembly for unzoned assemblies and because enrichment is ~6% greater than the assembly-average enrichment for zoned assemblies. This is expected to cause a ~1.8% bias in net neutron multiplication. The two assemblies (#1 and #2) without enrichment zoning exhibited a larger bias compared with most of the others in the analysed assembly set. The bias persisted even when the calculations were performed with the actual enrichment at the measurement position, suggesting that other sources of uncertainty may play a role. This observation is based on only two assemblies, and further investigation is needed to confirm the impact.

Calculations performed using the actual cycle history data (i.e., cycle dates and assembly power) had relatively little impact on the net neutron multiplication of the analysed assemblies. The primary fissionable nuclides have half-lives that are long compared with the operating history length, making the operating history second-order in importance for the net neutron multiplication. However, the operating histories can significantly affect the neutron and gamma count rates since in this case the half-lives of the important nuclides are relatively short.

An uncertainty assessment of the calculations was performed to estimate the potential impact of the accuracy and the completeness of declaration information on the simulated observables. Uncertainty in the burnup is one of the largest sources of modeling uncertainty. The calculation of net neutron multiplication is also subject to uncertainties due to approximations in the software algorithm. Specifically, leakage factors, which are used to account for the effect of assembly design on net neutron multiplication, are only currently available for the 8 × 8 and 10 × 10 SVEA designs, as calculated in this study. Such factors for other designs were not calculated and are assigned an approximate value from one of the two considered assembly designs. This assumption is estimated to introduce an uncertainty of 1–2% in net neutron multiplication. Developing additional leakage factors that are specific for the current inventory of BWR assembly designs in Finland will likely reduce the modeling error.

Furthermore, leakage factors are assumed to be constant for a given geometry and be independent of the fuel compositions (e.g., enrichment and burnup). Previous detailed studies have shown that leakage can vary by several percent as a function of enrichment and burnup. Further scoping studies would be required to assess whether adding leakage factors specific to fuel compositions would reduce the deviations currently observed between the measured PNAR ratio and the calculated net neutron multiplication.

In summary, based on comparisons between calculation and measurement, the results show that the ORIGEN Module can reasonably predict the PNAR neutron and gamma signals and the net neutron multiplication, which is expected to be correlated to the measured PNAR ratio. Because an ORIGEN Module calculation takes only seconds to complete, such predictions will be useful for the safeguards inspectors to draw conclusions in real time. Future work is recommended to develop leakage factors for other assembly types and to further improve the algorithm to calculate net neutron multiplication.

ACKNOWLEDGMENTS

This work was funded by the DOE/NNSA's International Nuclear Safeguards Engagement Program. The PNAR models and the measurement data were provided by Topi Tupasela of STUK (Finland), and the operator data were provided by Tommi Lamminpaa of TVO (Finland). The authors thank Steve Tobin of LANL, Tapani Honkamaa of STUK, and Marita Mosconi of Euratom for their valuable feedback.

REFERENCES

[1] S. Vaccaro, J. Hu, J. Svedkauskaite, A. Smejkal, P. Schwalbach, P. De Baere and I. C. Gauld, "A New Approach to Fork Measurements Data Analysis by RADAR-CRISP and ORIGEN Integration," *IEEE Trans. Nucl. Sci.*, vol. 61, no. 4, pp. 2161-2168, 2014. https://ieeexplore.ieee.org/document/6851223.

[2] "SCALE: A Comprehensive Modeling and Simulation Suite for Nuclear Safety Analysis and Design," ORNL/TM-2005/39, Version 6.1, Oak Ridge National Laboratory, 2011.

[3] S. Vaccaro, I. C. Gauld, J. Hu, P. De Baere, J. Peterson, P. Schwalbach, A. Smejkal, A. Tomanin, A. Sjöland, S. Tobin and D. Wiarda, "Advancing the Fork Detector for Quantitative Spent Nuclear

Fuel Verification," *Nuclear Inst. and Methods in Physics Research, A*, Vol. 888; pp. 202–217, 2018. https://doi.org/10.1016/j.nima.2018.01.066.

[4] J. Hu, I. C. Gauld, S. Vaccaro, T. Honkamaa and G. Ilas, "Validation of ORIGEN for VVER-440 Spent Fuel with Application to Fork Detector Safeguards Measurements," *ESARDA Bulletin*, no. 60, pp. 28-42, 2020. https://doi.org/10.2760/217080.

[5] M. A. Humphrey, S. J. Tobin and K. D. Veal, "The Next Generation Safeguards Initiative's Spent Fuel Nondestructive Assay Project," *Journal of Nuclear Materials Management*, vol. 40, no. 3, p. 6, 2012.

[6] S. J. Tobin, P. Peura, T. Honkamaa, P. Dendooven, M. Moring and C. Bélanger-Champagne, "Passive Neutron Albedo Reactivity in the Finnish Encapsulation Context," STUK report (Nuclear Materials), ISBN 978-952-309-406-2, 2018.

[7] T. Tupasela, S. J. Tobin, P. Dendooven and T. Honkamaa, "PNAR Measurement Report," STUK, Olkiluoto, Finland, 2019. https://doi.org/10.2172/1572311.

[8] W. A. Wieselquist, R. A. Lefebvre and M. A. Jessee (Editors), "SCALE Code System," ORNL/TM-2005/39, Version 6.2.4, Oak Ridge National Laboratory, Oak Ridge, TN, 2020. https://www.ornl.gov/file/scale-62-manual/display.

[9] D. B. Pelowitz (Editor), "MCNP6 USER'S MANUAL (version 1.0)," Los Alamos National Laboratory, LA-CP-13-00634, 2013.

[10] I. C. Gauld, D. Wiarda, J. Hu and K. Dugan, "ORIGEN Module for Fork Detector Data Analysis. Software Installation Guide and User Manual. Software Version 2.0.0," Oak Ridge National Laboratory, Oak Ridge, TN, 2018.

[11] I. C. Gauld and U. Mertyurek, "Validation of BWR spent nuclear fuel isotopic predictions with applications to burnup credit," *Nuclear Engineering and Design*, vol. 345, pp. 110-124, 2019. https://doi.org/10.1016/j.nucengdes.2019.01.026.

[12] W. Marshall, B. J. Ade, S. M. Bowman, I. C. Gauld, G. Ilas, U. Mertyurek and G. Radulescu, "Technical Basis for Peak Reactivity Burnup Credit for BWR Spent Nuclear Fuel in Storage and Transportation Systems," U.S. Nuclear Regulatory Commission, NUREG/CR-7194, 2015. http://www.nrc.gov/reading-rm/doc-collections/nuregs/contract/cr7194/.